

LEPTOGENESIS AND NEUTRINO MASSES IN AN INFLATIONARY SUSY PATI-SALAM MODEL

C. PALLIS AND N. TOUMBAS

*Department of Physics, University of Cyprus,
P.O. Box 20537, CY-1678 Nicosia, CYPRUS*

ABSTRACT

We implement the mechanism of non-thermal leptogenesis in the framework of an inflationary model based on a *supersymmetric* (SUSY) Pati-Salam *Grand Unified Theory* (GUT). In particular, we show that inflation is driven by a quartic potential associated with the Higgs fields involved in the spontaneous GUT symmetry breaking, in the presence of a non-minimal coupling of the inflaton field to gravity. The inflationary model relies on renormalizable superpotential terms and does not lead to overproduction of magnetic monopoles. It is largely independent of one-loop radiative corrections, and it can be consistent with current observational data on the inflationary observables, with the GUT symmetry breaking scale assuming its SUSY value. Non-thermal leptogenesis is realized by the out-of-equilibrium decay of the two lightest *right-handed* (RH) neutrinos, which are produced by the inflaton decay. Confronting our scenario with the current observational data on light neutrinos, the GUT prediction for the heaviest Dirac neutrino mass, the baryon asymmetry of the universe and the gravitino limit on the reheating temperature, we constrain the masses of the RH neutrinos in the range $(10^{10} - 10^{15})$ GeV and the Dirac neutrino masses of the two first generations to values between 0.1 and 20 GeV.

Keywords: Baryogenesis, Inflation, Grand Unified Theories

PACs Codes: 98.80.Cq, 11.30.Qc, 11.30.Er, 11.30.Pb, 12.60.Jv

1. INTRODUCTION

One of the most promising and well-motivated mechanisms for the generation of the *Baryon Asymmetry of the Universe* (BAU) is via an initial generation of a lepton asymmetry, which can be subsequently converted to BAU through sphaleron effects – see e.g. Ref. (1; 2). *Non-Thermal Leptogenesis* (nTL) (3; 4) is a variant of this proposal, in which the necessitated departure from equilibrium is achieved by construction. Namely, the *right-handed* (RH) neutrinos, ν_i^c , whose decay produces the lepton asymmetry, are out-of-equilibrium at the onset, since their masses are larger than the reheating temperature. Such a set-up can be achieved by the direct production of ν_i^c through the inflaton decay, which can also take place out-of-equilibrium.

Therefore, such a leptogenesis paradigm largely depends on the inflationary stage, which it follows.

In a recent paper (5) – for similar attempts, see Ref. (6–8) –, we investigate an inflationary model where a *Standard Model* (SM) singlet component of the Higgs fields involved in the spontaneous breaking of a *supersymmetric* (SUSY) *Pati-Salam* (PS) *Grand Unified Theory* (GUT) can produce inflation of chaotic-type, named *non-minimal Higgs Inflation* (nMHI), since there is a relatively strong non-minimal coupling of the inflaton field to gravity (9–12). This GUT provides a natural framework to implement our leptogenesis scenario, since the presence of the $SU(2)_R$ gauge symmetry predicts the existence of three ν_i^c . In its simplest realization this GUT leads to third family *Yukawa unification* (YU), and does not suffer from the doublet-triplet splitting problem since both Higgs doublets are contained in a bidoublet other than the GUT scale Higgs fields. Although this GUT is not completely unified – as, e.g., a GUT based on the $SO(10)$ gauge symmetry group – it emerges in standard weakly coupled heterotic string models (13) and in recent D-brane constructions (14).

The inflationary model relies on renormalizable superpotential terms and does not lead to overproduction of magnetic monopoles. It is largely independent of the one-loop radiative corrections (15), and it can become consistent with the fitting (16) of the seven-year data of the *Wilkinson Microwave Anisotropy Probe Satellite* (WMAP7) combined with the *baryon-acoustic oscillation* (BAO) and the measurement of the *Hubble constant* (H_0). At the same time the GUT symmetry breaking scale attains its SUSY value and the μ problem of the *Minimal SUSY SM* (MSSM) is resolved via a Peccei-Quinn (PQ) symmetry, solving also the strong CP problem. Inflation can be followed by non-thermal leptogenesis, compatible with the gravitino (\tilde{G}) limit (17–19) on the reheating temperature, leading to efficient baryogenesis. In Ref. (5) we connect non-thermal leptogenesis with neutrino data, implementing a two-generation formulation of the see-saw (20–22) mechanism and imposing extra restrictions from the data on the light neutrino masses and the GUT symmetry on the heaviest Dirac neutrino mass. There we (5) assume that the mixing angle between the first and third generation, θ_{13} , vanishes. However, the most updated (23; 24) analyses of the low energy neutrino data suggest that non-zero values for θ_{13} are now preferred, while the zero value can be excluded at 8 standard deviations. Therefore, a revision of our results, presented in Ref. (5), is worth pursuing.

The three-generation implementation of the see-saw mechanism is here adopted, following a bottom-up approach, along the lines of Ref. (25–28). In particular, we use as input parameters the low energy neutrino observables considering several schemes of neutrino masses. Using also the third generation Dirac neutrino mass predicted by the PS GUT, assuming a mild hierarchy for the two residual generations and imposing the restriction from BAU, we constrain the masses of ν_i^c 's and the residual neutrino Dirac mass spectrum. Renormalization group effects (28; 29) are also incorporated in our analysis.

We present the basic ingredients of our model in Sec. 2. In Sec. 3 we describe the inflationary potential and derive the inflationary observables. In Sec. 4 we outline the mechanism of non-thermal leptogenesis, while in Sec. 5 we exhibit the relevant imposed constraints and restrict the parameters of our model. Our conclusions are summarized in Sec. 6. Throughout the text, we use natural units for Planck's and Boltzmann's constants and the speed of light ($\hbar = c = k_B = 1$); the subscript of type $_{,\chi}$ denotes derivation *with respect to* (w.r.t) the field χ (e.g., $_{,\chi\chi} = \partial^2/\partial\chi^2$); charge conjugation is denoted by a star and $\log [\ln]$ stands for logarithm with basis 10 [e].

2. THE PATI-SALAM SUSY GUT MODEL

In this section, we present the particle content (Sec. 2.1), the structure of the superpotential and the Kähler potential (Sec. 2.2) and describe the SUSY limit (Sec. 2.3) of our model.

2.1 PARTICLE CONTENT

We focus on a SUSY PS GUT model described in detail in Ref. (5; 30). The representations and the transformation properties of the various superfields under $G_{PS} = SU(4)_C \times SU(2)_L \times SU(2)_R$, their decomposition under $G_{SM} = SU(3)_C \times SU(2)_L \times U(1)_Y$, as well as their extra global charges are presented in Table 1.

The i th generation ($i = 1, 2, 3$) *left-handed* (LH) quark and lepton superfields, u_{ia}, d_{ia} ($a = 1, 2, 3$ is a color index), e_i and ν_i are accommodated in a superfield F_i . The LH antiquark and antilepton superfields $u_{ia}^c, d_{ia}^c, e_i^c$ and ν_i^c are arranged in another superfield F_i^c . The gauge symmetry G_{PS} can be spontaneously broken down to G_{SM} through v.e.v.s which the superfields H^c and \bar{H}^c acquire in the directions ν_H^c and $\bar{\nu}_H^c$. The model also contains a gauge singlet S , which triggers the breaking of G_{PS} , as well as an $SU(4)_C$ 6-plet G , which splits into g_a^c and \bar{g}_a^c under G_{SM} and gives (13) superheavy masses to d_{Ha}^c and \bar{d}_{Ha}^c . In the simplest realization of this model (13; 30), the electroweak doublets H_u and H_d , which couple to the up and down quarks respectively, are exclusively contained in the bidoublet superfield H .

In addition to G_{PS} , the model possesses two global $U(1)$ symmetries, namely a PQ and an R symmetry, as well as a discrete \mathbb{Z}_2^{mp} symmetry ('matter parity') under which F, F^c change sign. The last symmetry forbids undesirable mixings of F and H and/or F^c and H^c and ensures the stability of the *lightest SUSY particle* (LSP). The imposed $U(1)$ R symmetry, $U(1)_R$, guarantees the linearity of the superpotential w.r.t the singlet S . Finally the $U(1)$ PQ symmetry, $U(1)_{PQ}$, assists us to generate the μ -term of the MSSM. The PQ breaking occurs at an intermediate scale through the v.e.v.s of P, \bar{P} , and the μ -term is generated via a non-renormalizable coupling of P and H . Following Ref. (30), we introduce into the scheme quartic (non-renormalizable) superpotential couplings of \bar{H}^c to F_i^c , which generate intermediate-scale masses for the ν_i^c and, thus, masses for the light neutrinos, ν_i , via the seesaw mechanism (20–22). Moreover, these couplings allow for the decay of the inflaton into ν_i^c , leading to a reheating temperature consistent with the \tilde{G} constraint with more or less natural values of the parameters. As shown finally in Ref. (30), the proton turns out to be practically stable in this model.

2.2 SUPERPOTENTIAL AND KÄHLER POTENTIAL

The superpotential W of our model splits into three parts:

$$W = W_{MSSM} + W_{PQ} + W_{HPS}, \quad (1)$$

which are analyzed in the following.

- W_{MSSM} is the part of W which contains the usual terms – except for the μ term – of the MSSM, supplemented by Yukawa interactions among the left-handed leptons and ν_i^c :

$$\begin{aligned} W_{MSSM} &= y_{ij} F_i H F_j^c = \\ &= y_{ij} \left(H_d^\top \varepsilon L_i e_j^c - H_u^\top \varepsilon L_i \nu_j^c + H_d^\top \varepsilon Q_{ia} d_{ja}^c - H_u^\top \varepsilon Q_{ia} u_{ja}^c \right), \quad \text{with } \varepsilon = \begin{pmatrix} 0 & 1 \\ -1 & 0 \end{pmatrix}. \end{aligned} \quad (2)$$

SUPER- FIELDS	REPRESE- NTATIONS	TRASFOR- MATIONS	DECOMPO- SITIONS	GLOBAL CHARGES		
	UNDER G_{PS}	UNDER G_{PS}	UNDER G_{SM}	R	PQ	\mathbb{Z}_2^{mp}
MATTER SUPERFIELDS						
F_i	$(\mathbf{4}, \mathbf{2}, \mathbf{1})$	$F_i U_{\text{L}}^{\dagger} U_{\text{C}}^{\text{T}}$	$Q_{ia}(\mathbf{3}, \mathbf{2}, 1/6)$ $L_i(\mathbf{1}, \mathbf{2}, -1/2)$	1	-1	-
F_i^c	$(\bar{\mathbf{4}}, \mathbf{1}, \mathbf{2})$	$U_{\text{C}}^* U_{\text{R}}^* F_i^c$	$u_{ia}^c(\bar{\mathbf{3}}, \mathbf{1}, -2/3)$ $d_{ia}^c(\bar{\mathbf{3}}, \mathbf{1}, 1/3)$ $\nu_i^c(\mathbf{1}, \mathbf{1}, 0)$ $e_i^c(\mathbf{1}, \mathbf{1}, 1)$	1	0	-
HIGGS SUPERFIELDS						
H^c	$(\bar{\mathbf{4}}, \mathbf{1}, \mathbf{2})$	$U_{\text{C}}^* U_{\text{R}}^* H^c$	$u_{\text{Ha}}^c(\bar{\mathbf{3}}, \mathbf{1}, -2/3)$ $d_{\text{Ha}}^c(\bar{\mathbf{3}}, \mathbf{1}, 1/3)$ $\nu_H^c(\mathbf{1}, \mathbf{1}, 0)$ $e_H^c(\mathbf{1}, \mathbf{1}, 1)$	0	0	+
\bar{H}^c	$(\mathbf{4}, \mathbf{1}, \mathbf{2})$	$\bar{H}^c U_{\text{R}}^{\text{T}} U_{\text{C}}^{\text{T}}$	$\bar{u}_{\text{Ha}}^c(\mathbf{3}, \mathbf{1}, 2/3)$ $\bar{d}_{\text{Ha}}^c(\mathbf{3}, \mathbf{1}, -1/3)$ $\bar{\nu}_H^c(\mathbf{1}, \mathbf{1}, 0)$ $\bar{e}_H^c(\mathbf{1}, \mathbf{1}, -1)$	0	0	+
S	$(\mathbf{1}, \mathbf{1}, \mathbf{1})$	S	$S(\mathbf{1}, \mathbf{1}, 0)$	2	0	+
G	$(\mathbf{6}, \mathbf{1}, \mathbf{1})$	$U_{\text{C}} G U_{\text{C}}^{\text{T}}$	$\bar{g}_{\text{a}}^c(\mathbf{3}, \mathbf{1}, -1/3)$ $g_{\text{a}}^c(\bar{\mathbf{3}}, \mathbf{1}, 1/3)$	2	0	+
H	$(\mathbf{1}, \mathbf{2}, \mathbf{2})$	$U_{\text{L}} H U_{\text{R}}^{\text{T}}$	$H_u(\mathbf{1}, \mathbf{2}, 1/2)$ $H_d(\mathbf{1}, \mathbf{2}, -1/2)$	0	1	+
P	$(\mathbf{1}, \mathbf{1}, \mathbf{1})$	P	$P(\mathbf{1}, \mathbf{1}, 0)$	1	-1	+
\bar{P}	$(\mathbf{1}, \mathbf{1}, \mathbf{1})$	\bar{P}	$\bar{P}(\mathbf{1}, \mathbf{1}, 0)$	0	1	+

TABLE 1. The representations, the transformations under G_{PS} , the decompositions under G_{SM} as well as the extra global charges of the superfields of our model. Here $U_C \in SU(4)_C$, $U_L \in SU(2)_L$, $U_R \in SU(2)_R$ and \dagger , \dagger and $*$ stand for the transpose, the hermitian conjugate and the complex conjugate of a matrix respectively.

Here $Q_{ia} = \begin{pmatrix} u_{ia} & d_{ia} \end{pmatrix}^\top$ and $L_i = \begin{pmatrix} \nu_i & e_i \end{pmatrix}^\top$ are the i -th generation $SU(2)_L$ doublet LH quark and lepton superfields respectively. Summation over repeated color and generation indices is assumed. Obviously the model predicts YU at M_{GUT} since the fermion masses per family originate from a unique term of the PS GUT. It is shown (31; 32) that exact third family YU combined with non-universalities in the gaugino sector and/or the scalar sector can become consistent with a number of phenomenological and cosmological low-energy requirements. On the other hand, it is expected on generic grounds that the predictions of this simple model for the fermion masses of the two lighter generations are not valid. Usually this difficulty can be avoided by introducing (33) an abelian symmetry which establishes a hierarchy between the flavor dependent couplings. Alternatively, the present

model can be augmented (34) with other Higgs fields so that H_u and H_d are not exclusively contained in H , but receive subdominant contributions from other representations too. As a consequence, a moderate violation of exact YU can be achieved, allowing for an acceptable low-energy phenomenology, even with universal boundary conditions for the soft SUSY breaking terms. However, we prefer here to work with the simplest version of the PS model, using the prediction of the third family YU in order to determine the corresponding Dirac neutrino mass – see Sec. 5.1.

- W_{PQ} , is the part of W which is relevant for the spontaneous breaking of $U(1)_{\text{PQ}}$ and the generation of the μ term of the MSSM. It is given by

$$W_{\text{PQ}} = \lambda_{\text{PQ}} \frac{P^2 \bar{P}^2}{M_S} - \lambda_\mu \frac{P^2}{2M_S} \text{Tr} \left(H \epsilon H^\top \epsilon \right), \quad (3)$$

where $M_S \simeq 5 \cdot 10^{17}$ GeV is the String scale. The scalar potential, which is generated by the first term in the RHS of Eq. (3), after gravity-mediated SUSY breaking, is studied in Ref. (30; 35). For a suitable choice of parameters, the minimum lies at $|\langle P \rangle| = |\langle \bar{P} \rangle| \sim \sqrt{m_{3/2} M_S}$. Hence, the PQ symmetry breaking scale is of order $\sqrt{m_{3/2} M_S} \simeq (10^{10} - 10^{11})$ GeV. The μ -term of the MSSM is generated from the second term of the RHS of Eq. (3) as follows:

$$- \lambda_\mu \frac{\langle P \rangle^2}{2M_S} \text{Tr} \left(H \epsilon H^\top \epsilon \right) = \mu H_d^\top \epsilon H_u \Rightarrow \mu \simeq \lambda_\mu \frac{\langle P \rangle^2}{M_S}, \quad (4)$$

which is of the right magnitude if $\lambda_\mu \sim (0.001 - 0.01)$. Let us note that V_{PQ} has an additional local minimum at $P = \bar{P} = 0$, which is separated from the global PQ minimum by a sizable potential barrier, thus preventing transitions from the trivial to the PQ vacuum. Since this situation persists at all cosmic temperatures after reheating, we are obliged to assume that, after the termination of nMHI, the system emerges with the appropriate combination of initial conditions so that it is led (36) in the PQ vacuum.

- W_{HPS} , is the part of W which is relevant for nMHI, the spontaneous breaking of G_{PS} and the generation of intermediate Majorana [superheavy] masses for ν_i^c [d_H^c and \bar{d}_H^c]. It takes the form

$$W_{\text{HPS}} = \lambda S \left(\bar{H}^c H^c - M_{\text{PS}}^2 \right) + \lambda_H H^c \bar{G}^\top \epsilon H^c + \lambda_{\bar{H}} \bar{H}^c \bar{G} \epsilon \bar{H}^\top + \lambda_{\nu^c} \frac{(\bar{H}^c F_i^c)^2}{M_S}, \quad (5)$$

where M_{PS} is a superheavy mass scale related to M_{GUT} – see Sec. 3.2 – and \bar{G} is the dual tensor of G . The parameters λ and M_{PS} can be made positive by field redefinitions.

According to the general recipe (11; 12), the implementation of nMHI within SUGRA requires the adoption of a Kähler potential, K , of the following type

$$K = -3m_{\text{P}}^2 \ln \left(1 - \frac{H^c H^c}{3m_{\text{P}}^2} - \frac{\bar{H}^c \bar{H}^c}{3m_{\text{P}}^2} - \frac{\text{Tr} (G^\dagger G)}{6m_{\text{P}}^2} - \frac{|S|^2}{3m_{\text{P}}^2} + k_S \frac{|S|^4}{3m_{\text{P}}^4} + \frac{k_H}{2m_{\text{P}}^2} (H^c H^c + \text{h.c.}) \right), \quad (6)$$

where $m_{\text{P}} = 2.44 \cdot 10^{18}$ GeV is the reduced Planck scale and the complex scalar components of the superfields H^c , \bar{H}^c , G and S are denoted by the same symbol. The coefficients k_S and k_H are taken real. From Eq. (6) we can infer that we adopt the standard quadratic non-minimal coupling for Higgs-inflaton, which respects the gauge and global symmetries of the model.

This non-minimal coupling of the Higgs fields to gravity is transparent in the Jordan frame. We also added the fifth term in the RHS of Eq. (6) in order to cure the tachyonic mass problem encountered in similar models (10–12) – see Sec. 3.1. In terms of the components of the various fields, K in Eq. (6) reads

$$K = -3m_{\text{P}}^2 \ln \left(1 - \frac{\phi^\alpha \phi^{*\bar{\alpha}}}{3m_{\text{P}}^2} + k_S \frac{|S|^4}{3m_{\text{P}}^4} + \frac{k_H}{2m_{\text{P}}^2} (\nu_H^c \bar{\nu}_H^c + e_H^c \bar{e}_H^c + u_H^c \bar{u}_H^c + d_H^c \bar{d}_H^c + \text{h.c.}) \right) \quad (7a)$$

with

$$\phi^\alpha = \nu_H^c, \bar{\nu}_H^c, e_H^c, \bar{e}_H^c, u_H^c, \bar{u}_H^c, d_H^c, \bar{d}_H^c, g^c, \bar{g}^c \text{ and } S \quad (7b)$$

and summation over the repeated Greek indices is implied.

2.3 THE SUSY LIMIT

In the limit where m_{P} tends to infinity, we can obtain the SUSY limit of the SUGRA potential. Assuming that the SM non-singlet components vanish, the F-term potential in this limit, V_{F} , turns out to be

$$V_{\text{F}} = \lambda^2 \left| \bar{\nu}_H^c \nu_H^c - M_{\text{PS}}^2 \right|^2 + \lambda^2 |S|^2 \left(|\nu_H^c|^2 + |\bar{\nu}_H^c|^2 \right), \quad (8a)$$

while the D-term potential is

$$V_{\text{D}} = \frac{5g^2}{16} \left(|\nu_H^c|^2 - |\bar{\nu}_H^c|^2 \right)^2. \quad (8b)$$

Restricting ourselves to the D-flat direction $|\nu_H^c| = |\bar{\nu}_H^c|$, we find from V_{F} that the SUSY vacuum lies at

$$\langle S \rangle \simeq 0 \text{ and } |\langle \nu_H^c \rangle| = |\langle \bar{\nu}_H^c \rangle| = M_{\text{PS}}. \quad (9)$$

Therefore, W_{HPS} leads to spontaneous breaking of G_{PS} . As we shall see in Sec. 3, the same superpotential, W_{HPS} , gives rise to a stage of nMHI. Indeed, along the D-flat direction $|\nu_H^c| = |\bar{\nu}_H^c| \gg M_{\text{PS}}$ and $S = 0$, V_{SUSY} tends to a quartic potential, which can be employed in conjunction with K in Eq. (6) for the realization of nMHI along the lines of Ref. (12).

It should be mentioned that soft SUSY breaking and instanton effects explicitly break $U(1)_R \times U(1)_{\text{PQ}}$ to $\mathbb{Z}_2 \times \mathbb{Z}_6$. The latter symmetry is spontaneously broken by $\langle P \rangle$ and $\langle \bar{P} \rangle$. This would lead to a domain wall problem if the PQ transition took place after nMHI. However, as we already mentioned above, $U(1)_{\text{PQ}}$ is assumed already broken before or during nMHI. The final unbroken symmetry of the model is $G_{\text{SM}} \times \mathbb{Z}_2^{\text{mp}}$.

3. THE INFLATIONARY SCENARIO

Next we outline the salient features of our inflationary scenario (Sec. 3.1) and calculate a number of observable quantities in Sec. 3.2.

3.1 STRUCTURE OF THE INFLATIONARY POTENTIAL

At tree-level the *Einstein Frame* (EF) SUGRA potential, \hat{V}_{HI} , is given by (11)

$$\hat{V}_{\text{HI}} = e^{K/m_{\text{P}}^2} \left(K^{\alpha\bar{\beta}} F_\alpha F_{\bar{\beta}} - 3 \frac{|W_{\text{HPS}}|^2}{m_{\text{P}}^2} \right) + \frac{1}{2} g^2 \sum_a D_a D_a, \quad (10a)$$

where g is the unified gauge coupling constant and the summation is applied over the 21 generators T_a of the PS gauge group – see Ref. (5). Also, we have

$$K_{\alpha\bar{\beta}} = K_{\phi^a\phi^{*\bar{a}}}, \quad K^{\bar{\beta}\alpha}K_{\alpha\bar{\gamma}} = \delta_{\bar{\gamma}}^{\bar{\beta}}, \quad F_{\alpha} = W_{\text{HPS},\phi^a} + K_{\phi^a}W_{\text{HPS}}/m_{\text{P}}^2 \quad \text{and} \quad D_a = \phi_{\alpha}(T_a)^{\alpha}_{\bar{\beta}}K^{\bar{\beta}} \quad (10b)$$

The ϕ^{α} 's are given in Eq. (7b). If we parameterize the SM singlet components of H^c and \bar{H}^c by

$$\nu_H^c = h e^{i\theta} \cos \theta_v / \sqrt{2} \quad \text{and} \quad \bar{\nu}_H^c = h e^{i\bar{\theta}} \sin \theta_v / \sqrt{2}, \quad (11)$$

we can easily deduce that a D-flat direction occurs at

$$\theta = \bar{\theta} = 0, \quad \theta_v = \pi/4 \quad \text{and} \quad e_H^c = \bar{e}_H^c = u_H^c = \bar{u}_H^c = d_H^c = \bar{d}_H^c = g^c = \bar{g}^c = 0. \quad (12)$$

Along this direction, the D-terms in Eq. (10a) – and, also, V_D in Eq. (8b) – vanish, and so \hat{V}_{HI} takes the form

$$\hat{V}_{\text{HI}} = m_{\text{P}}^4 \frac{\lambda^2 (x_h^2 - 4m_{\text{PS}}^2)^2}{16f^2} \quad (13)$$

with

$$f = 1 + c_{\mathcal{R}} x_h^2, \quad m_{\text{PS}} = \frac{M_{\text{PS}}}{m_{\text{P}}}, \quad x_h = \frac{h}{m_{\text{P}}} \quad \text{and} \quad c_{\mathcal{R}} = -\frac{1}{6} + \frac{k_H}{4}. \quad (14)$$

From Eq. (13), we can verify that for $c_{\mathcal{R}} \gg 1$ and $m_{\text{PS}} \ll 1$, \hat{V}_{HI} takes a form suitable for the realization of nMHI, since it develops a plateau – see also Sec. 3.2. The (almost) constant potential energy density $\hat{V}_{\text{HI}0}$ and the corresponding Hubble parameter \hat{H}_{HI} (along the trajectory in Eq. (12)) are given by

$$\hat{V}_{\text{HI}0} = \frac{\lambda^2 h^4}{16f^2} \simeq \frac{\lambda^2 m_{\text{P}}^4}{16c_{\mathcal{R}}^2} \quad \text{and} \quad \hat{H}_{\text{HI}} = \frac{\hat{V}_{\text{HI}0}^{1/2}}{\sqrt{3}m_{\text{P}}} \simeq \frac{\lambda m_{\text{P}}}{4\sqrt{3}c_{\mathcal{R}}}. \quad (15)$$

We next proceed to check the stability of the trajectory in Eq. (12) w.r.t the fluctuations of the various fields. To this end, we expand them in real and imaginary parts as follows

$$X = \frac{x_1 + ix_2}{\sqrt{2}}, \quad \bar{X} = \frac{\bar{x}_1 + i\bar{x}_2}{\sqrt{2}} \quad \text{where} \quad X = e_H^c, u_H^c, d_H^c, g^c \quad \text{and} \quad x = e, u, d, g. \quad (16)$$

Notice that the field S can be rotated to the real axis via a suitable R transformation. Along the trajectory in Eq. (12) we find

$$(K_{\alpha\bar{\beta}}) = \text{diag} \left(\frac{M_K}{\bar{f}^2}, \underbrace{\frac{1}{\bar{f}}, \dots, \frac{1}{\bar{f}}}_{3+6 \cdot 3 \text{ times}} \right) \quad \text{with} \quad M_K = \begin{pmatrix} \kappa & \bar{\kappa} \\ \bar{\kappa} & \kappa \end{pmatrix}, \quad \bar{\kappa} = 3c_{\mathcal{R}}^2 x_h^2 \quad \text{and} \quad \kappa = f + \bar{\kappa}. \quad (17)$$

To canonically normalize the fields ν_H^c and $\bar{\nu}_H^c$, we first diagonalize the matrix M_K . This can be achieved via a similarity transformation involving an orthogonal matrix U_K as follows:

$$U_K M_K U_K^T = \text{diag}(\bar{f}, \bar{f}), \quad \text{where} \quad \bar{f} = f + 6c_{\mathcal{R}}^2 x_h^2 \quad \text{and} \quad U_K = \frac{1}{\sqrt{2}} \begin{pmatrix} 1 & 1 \\ -1 & 1 \end{pmatrix}. \quad (18)$$

Utilizing U_K , the kinetic terms of the various fields can be brought into the following form

$$K_{\alpha\bar{\beta}}\dot{\phi}^\alpha\dot{\phi}^{*\bar{\beta}} = \frac{\bar{f}}{2f^2} \left(\dot{h}^2 + \frac{1}{2}h^2\dot{\theta}_+^2 \right) + \frac{h^2}{2f} \left(\frac{1}{2}\dot{\theta}_-^2 + \dot{\theta}_v^2 \right) + \frac{1}{2f}\dot{\chi}_\alpha\dot{\chi}_\alpha = \frac{1}{2}\dot{\hat{h}}^2 + \frac{1}{2}\dot{\hat{\psi}}_\alpha\dot{\hat{\psi}}_\alpha, \quad (19)$$

where $\theta_\pm = (\bar{\theta} \pm \theta) / \sqrt{2}$, $\chi_\alpha = x_1, x_2, \bar{x}_1, \bar{x}_2, S$ and $\psi_\alpha = \theta_+, \theta_-, \theta_v, \chi_\alpha$ and the dot denotes derivation w.r.t the cosmic time, t . In the last line, we introduce the EF canonically normalized fields, \hat{h} and $\hat{\psi}$, which can be obtained as follows – cf. Ref. (5; 11; 12; 37):

$$\frac{d\hat{h}}{dt} = J = \frac{\sqrt{\bar{f}}}{f}, \quad \hat{\theta}_+ = \frac{Jh\theta_+}{\sqrt{2}}, \quad \hat{\theta}_- = \frac{h\theta_-}{\sqrt{2f}}, \quad \hat{\theta}_v = \frac{h}{\sqrt{f}} \left(\theta_v - \frac{\pi}{4} \right) \quad \text{and} \quad \hat{\chi}_\alpha = \frac{\chi_\alpha}{\sqrt{f}}. \quad (20)$$

Taking into account the approximate expressions for \hat{h} , J and the slow-roll parameters $\hat{\epsilon}$, $\hat{\eta}$, which are displayed in Sec. 3.2, we can verify that, during a stage of slow-roll inflation, $\hat{\theta}_+ \simeq Jh\theta_+/\sqrt{2}$ since $Jh \simeq \sqrt{6}m_P$, $\hat{\theta}_- \simeq h\theta_-/\sqrt{2f}$ and $\hat{\theta}_v \simeq h\theta_v/\sqrt{f}$ since $h/\sqrt{f} \simeq m_P/\sqrt{c_R}$. On the other hand, we can show that $\hat{\chi}_\alpha \simeq \chi_\alpha/\sqrt{f}$, since the quantity $\dot{f}/2f^{3/2}\chi_\alpha$, involved in relating $\dot{\chi}_\alpha$ to $\dot{\hat{\chi}}_\alpha$, turns out to be negligibly small compared with $\dot{\hat{\chi}}_\alpha$. Indeed, the $\hat{\chi}_\alpha$'s acquire effective masses $m_{\hat{\chi}_\alpha} \gg \hat{H}_{\text{HI}}$ – see below – and therefore enter a phase of oscillations about $\hat{\chi}_\alpha = 0$ with decreasing amplitude. Neglecting the oscillatory part of the relevant solutions, we find

$$\chi \simeq \hat{\chi}_{\alpha 0} \sqrt{f} e^{-2\hat{N}/3} \quad \text{and} \quad \dot{\hat{\chi}}_\alpha \simeq -2\chi_{\alpha 0} \sqrt{f} \hat{H}_{\text{HI}} \hat{\eta}_{\chi_\alpha} e^{-2\hat{N}/3}, \quad (21)$$

where $\hat{\chi}_{\alpha 0}$ represents the initial amplitude of the oscillations, $\hat{\eta}_{\chi_\alpha} = m_{\hat{\chi}_\alpha}^2/3\hat{H}_{\text{HI}}$ and we assume $\dot{\hat{\chi}}_\alpha(t=0) = 0$. Taking into account the approximate expressions for \hat{h} and the slow-roll parameter $\hat{\epsilon}$ in Sec. 3.2, we find

$$-\dot{f}/2f^{3/2}\chi_\alpha = \left(c_R \hat{\epsilon} \hat{H}_{\text{HI}}^2 / m_{\hat{\chi}_\alpha}^2 \right) \dot{\hat{\chi}}_\alpha \ll \dot{\hat{\chi}}_\alpha. \quad (22)$$

Having defined the canonically normalized scalar fields, we can proceed in investigating the stability of the inflationary trajectory of Eq. (12). To this end, we expand \hat{V}_{HI} in Eq. (10a) to quadratic order in the fluctuations around the direction of Eq. (12), as described in detail in Ref. (5). In Table 2 we list the eigenvalues of the mass-squared matrices

$$M_{\alpha\beta}^2 = \left. \frac{\partial^2 \hat{V}_{\text{HI}}}{\partial \hat{\psi}_\alpha \partial \hat{\psi}_\beta} \right|_{\text{Eq. (12)}} \quad \text{with} \quad \psi_\alpha = \theta_+, \theta_-, \theta_v, x_1, x_2, \bar{x}_1, \bar{x}_2 \quad \text{and} \quad S \quad (23)$$

involved in the expansion of \hat{V}_{HI} . We arrange our findings into three groups: the SM singlet sector, $S - \nu_H^c - \bar{\nu}_H^c$, the sector with the u_H^c, \bar{u}_H^c and the e_H^c, \bar{e}_H^c fields which are related with the broken generators of G_{PS} and the sector with the d_H^c, \bar{d}_H^c and the g^c, \bar{g}^c fields. Upon diagonalization of the relevant matrices we obtain the following mass eigenstates:

$$\hat{x}_{1\pm} = \frac{1}{\sqrt{2}} (\hat{x}_1 \pm \hat{x}_1) \quad \text{and} \quad \hat{x}_{2\mp} = \frac{1}{\sqrt{2}} (\hat{x}_2 \mp \hat{x}_2) \quad \text{with} \quad x = u, e, d \quad \text{and} \quad g. \quad (24)$$

As we observe from the relevant eigenvalues, no instability – as the one found in Ref. (37) – arises in the spectrum. In particular, it is evident that $k_S \gtrsim 1$ assists us to achieve $m_S^2 > 0$

FIELDS	MASSES SQUARED	EIGENSTATES
THE $S - \nu_H^c - \bar{\nu}_H^c$ SECTOR		
2 real scalars	$m_{\hat{\theta}_\nu}^2 = m_{\mathbb{P}}^2 x_h^2 (2\lambda^2(x_h^2 - 6) + 15g^2 f) / 24f^2$	$\hat{\theta}_\nu$
	$m_{\hat{\theta}_+}^2 = \lambda^2 m_{\mathbb{P}}^4 x_h^2 (1 + 6c_{\mathcal{R}}) / 12f^2 f^3 \simeq 4\hat{H}_{\text{HI}}^2$	$\hat{\theta}_+$
1 complex scalar	$m_{\hat{S}}^2 = \lambda^2 m_{\mathbb{P}}^2 x_h^2 (12 + x_h^2 \bar{f}) (6k_S f - 1) / 6f^2 \bar{f}$	\hat{S}
THE $u_{Ha}^c - \bar{u}_{Ha}^c$ ($a = 1, 2, 3$) AND $e_H^c - \bar{e}_H^c$ SECTORS		
2(3 + 1) real scalars	$m_{\hat{u}_-}^2 = m_{\mathbb{P}}^2 x_h^2 (\lambda^2(x_h^2 - 3) + 3g^2 f) / 12f^2$ $m_{\hat{e}_-}^2 = m_{\hat{u}_-}^2$	$\hat{u}_{1-}^a, \hat{u}_{2+}^a,$ $\hat{e}_{1-}, \hat{e}_{2+}$
THE $d_{Ha}^c - \bar{d}_{Ha}^c$ AND $g_a^c - \bar{g}_a^c$ ($a = 1, 2, 3$) SECTORS		
3 · 8 real scalars	$m_{\hat{g}}^2 = m_{\mathbb{P}}^2 x_h^2 (\lambda^2 x_h^2 + 24\lambda_H^2 f) / 24f^2$ $m_{\hat{g}}^2 = m_{\mathbb{P}}^2 x_h^2 (\lambda^2 x_h^2 + 24\lambda_H^2 f) / 24f^2$ $m_{\hat{d}_+}^2 = m_{\mathbb{P}}^2 x_h^2 (\lambda^2 + 4\lambda_H^2 f) / 4f^2$ $m_{\hat{d}_-}^2 = m_{\mathbb{P}}^2 x_h^2 (\lambda^2 (x_h^2 - 3) + 12\lambda_H^2 f) / 12f^2$	\hat{g}_1^a, \hat{g}_2^a \hat{g}_1^a, \hat{g}_2^a $\hat{d}_{1+}^a, \hat{d}_{2-}^a$ $\hat{d}_{1-}^a, \hat{d}_{2+}^a$

TABLE 2. The scalar mass spectrum of our model along the inflationary trajectory of Eq. (12). To avoid very lengthy formulas we neglect terms proportional to $m_{\mathbb{P}}^2$ and we assume $\lambda_H \simeq \lambda_{\mathbb{H}}$ for the derivation of the masses of the scalars in the superfields $d_{H\bar{a}}^c$ and $\bar{d}_{H\bar{a}}^c$.

– in accordance with the results of Ref. (12). Moreover, the D-term contributions to $m_{\hat{\theta}_\nu}^2$ and $m_{\hat{u}_-}^2$ – proportional to the gauge coupling constant $g \simeq 0.7$ – ensure the positivity of these masses squared. Finally the masses that the scalars $\hat{d}_{1,2}$ acquire from the second and third term of the RHS of Eq. (5) lead to the positivity of $m_{\hat{d}_-}^2$ for λ_H of order unity. We have also numerically verified that the masses of the various scalars remain greater than the Hubble parameter during the last 50 – 60 e-foldings of nMHI, and so any inflationary perturbations of the fields other than the inflaton are safely eliminated.

The 8 Goldstone bosons, associated with the modes \hat{x}_{1+} and \hat{x}_{2-} with $x = u^a$ and e , are not exactly massless since $\hat{V}_{\text{HI},h} \neq 0$ – contrary to the situation of Ref. (30) where the direction with non vanishing $\langle \nu_H^c \rangle$ minimizes the potential. These masses turn out to be $m_{x0} = \lambda m_{\mathbb{P}} x_h / 2f$. On the contrary, the angular parametrization in Eq. (11) assists us to isolate the massless mode $\hat{\theta}_-$, in agreement with the analysis of Ref. (11). Employing the well-known Coleman-Weinberg formula (15), we can compute the one-loop radiative corrections to the potential in our model. However, these have no significant effect on the inflationary dynamics and predictions, since the slope of the inflationary path is generated at the classical level – see the expressions for \hat{e} and $\hat{\eta}$ below.

3.2 THE INFLATIONARY OBSERVABLES

Based on the potential of Eq. (13) and keeping in mind that the EF canonically inflaton \hat{h} is related to h via Eq. (20), we can proceed to the analysis of nMHI in the EF, employing the

standard slow-roll approximation. Namely, a stage of slow-roll nMHI is determined by the condition – see e.g. Ref. (38; 39):

$$\max\{\hat{\epsilon}(h), |\hat{\eta}(h)|\} \leq 1,$$

where

$$\hat{\epsilon} = \frac{m_{\text{P}}^2}{2} \left(\frac{\hat{V}_{\text{HI},\hat{h}}}{\hat{V}_{\text{HI}}} \right)^2 = \frac{m_{\text{P}}^2}{2J^2} \left(\frac{\hat{V}_{\text{HI},h}}{\hat{V}_{\text{HI}}} \right)^2 \simeq \frac{4f_0^2 m_{\text{P}}^4}{3c_{\mathcal{R}}^2 h^4} \quad (25a)$$

and

$$\hat{\eta} = m_{\text{P}}^2 \frac{\hat{V}_{\text{HI},\hat{h}\hat{h}}}{\hat{V}_{\text{HI}}} = \frac{m_{\text{P}}^2}{J^2} \left(\frac{\hat{V}_{\text{HI},hh}}{\hat{V}_{\text{HI}}} - \frac{\hat{V}_{\text{HI},h}}{\hat{V}_{\text{HI}}} \frac{J_{,h}}{J} \right) \simeq -\frac{4f_0 m_{\text{P}}^2}{3c_{\mathcal{R}} h^2}, \quad (25b)$$

are the slow-roll parameters and $f_0 = f(\langle h \rangle = 2M_{\text{PS}}) = 1 + 4c_{\mathcal{R}} m_{\text{PS}}^2$ – see Sec. 4.1. Here we employ Eq. (15) and the following approximate relations:

$$J \simeq \sqrt{6} \frac{m_{\text{P}}}{h}, \quad \hat{V}_{\text{HI},h} \simeq \frac{4\hat{V}_{\text{HI}}}{c_{\mathcal{R}} h^3} f_0 m_{\text{P}}^2 \quad \text{and} \quad \hat{V}_{\text{HI},hh} \simeq -\frac{12\hat{V}_{\text{HI}}}{c_{\mathcal{R}} h^4} f_0 m_{\text{P}}^2. \quad (26)$$

The numerical computation reveals that nMHI terminates due to the violation of the $\hat{\epsilon}$ criterion at a value of h equal to h_{f} , which is calculated to be

$$\hat{\epsilon}(h_{\text{f}}) = 1 \Rightarrow h_{\text{f}} = (4/3)^{1/4} m_{\text{P}} \sqrt{f_0/c_{\mathcal{R}}}. \quad (27)$$

The number of e-foldings, \hat{N}_* , that the scale $k_* = 0.002/\text{Mpc}$ suffers during nMHI can be calculated through the relation:

$$\hat{N}_* = \frac{1}{m_{\text{P}}^2} \int_{\hat{h}_{\text{f}}}^{\hat{h}_*} d\hat{h} \frac{\hat{V}_{\text{HI}}}{\hat{V}_{\text{HI},\hat{h}}} = \frac{1}{m_{\text{P}}^2} \int_{h_{\text{f}}}^{h_*} dh J^2 \frac{\hat{V}_{\text{HI}}}{\hat{V}_{\text{HI},h}}, \quad (28)$$

where $h_* [\hat{h}_*]$ is the value of $h [\hat{h}]$ when k_* crosses the inflationary horizon. Given that $h_{\text{f}} \ll h_*$, we can write h_* as a function of \hat{N}_* as follows

$$\hat{N}_* \simeq \frac{3c_{\mathcal{R}}}{4f_0} \frac{h_*^2 - h_{\text{f}}^2}{m_{\text{P}}^2} \Rightarrow h_* = 2m_{\text{P}} \sqrt{\hat{N}_* f_0 / 3c_{\mathcal{R}}}. \quad (29)$$

The power spectrum $\Delta_{\mathcal{R}}^2$ of the curvature perturbations generated by h at the pivot scale k_* is estimated as follows

$$\Delta_{\mathcal{R}} = \frac{1}{2\sqrt{3} \pi m_{\text{P}}^3} \frac{\hat{V}_{\text{HI}}(\hat{h}_*)^{3/2}}{|\hat{V}_{\text{HI},\hat{h}}(\hat{h}_*)|} \simeq \frac{\lambda h_*^2}{16\sqrt{2} \pi f_0 m_{\text{P}}^2} \simeq \frac{\lambda \hat{N}_*}{12\sqrt{2} \pi c_{\mathcal{R}}}. \quad (30)$$

Since the scalars listed in Table 2 are massive enough during nMHI, $\Delta_{\mathcal{R}}$ can be identified with its central observational value – see Sec. 5 – with almost constant \hat{N}_* . The resulting relation reveals that λ is to be proportional to $c_{\mathcal{R}}$. Indeed we find

$$\lambda \simeq 8.4 \cdot 10^{-4} \pi c_{\mathcal{R}} / \hat{N}_* \Rightarrow c_{\mathcal{R}} \simeq 20925 \lambda \quad \text{for} \quad \hat{N}_* \simeq 55. \quad (31)$$

The (scalar) spectral index n_s , its running a_s , and the scalar-to-tensor ratio r can be estimated through the relations:

$$n_s = 1 - 6\hat{\epsilon}_* + 2\hat{\eta}_* \simeq 1 - 2/\hat{N}_*, \quad (32a)$$

$$\alpha_s = \frac{2}{3} \left(4\hat{\eta}_*^2 - (n_s - 1)^2 \right) - 2\hat{\xi}_* \simeq -2\hat{\xi}_* \simeq -2/\hat{N}_*^2 \quad (32b)$$

and

$$r = 16\hat{\epsilon}_* \simeq 12/\hat{N}_*^2, \quad (32c)$$

where $\hat{\xi} = m_P^4 \hat{V}_{\text{HI},h} \hat{V}_{\text{HI},\widetilde{hh}} / \hat{V}_{\text{HI}}^2 = m_P \sqrt{2\hat{\epsilon}} \hat{\eta}_{,h} / J + 2\hat{\eta}\hat{\epsilon}$. The variables with subscript $*$ are evaluated at $h = h_*$ and Eqs. (25a) and (25b) have been employed.

4. NON-THERMAL LEPTOGENESIS

In this section, we specify how the SUSY inflationary scenario makes a transition to the radiation dominated era (Sec. 4.1) and give an explanation of the origin of the observed BAU (Sec. 4.2) consistently with the \tilde{G} constraint and the low energy neutrino data (Sec. 4.3).

4.1 THE INFLATON'S DECAY

When nMHI is over, the inflaton continues to roll down towards the SUSY vacuum, Eq. (9). There is a brief stage of tachyonic preheating (40) which does not lead to significant particle production (41). Soon after, the inflaton settles into a phase of damped oscillations initially around zero – where $\hat{V}_{\text{HI}0}$ has a maximum – and then around one of the minima of $\hat{V}_{\text{HI}0}$. Whenever the inflaton passes through zero, particle production may occur creating mostly superheavy bosons via the mechanism of instant preheating (42). This process becomes more efficient as λ decreases, and further numerical investigation is required in order to check the viability of the non-thermal leptogenesis scenario for small values of λ . For this reason, we restrict to λ 's larger than 0.001, which ensures a less frequent passage of the inflaton through zero, weakening thereby the effects from instant preheating and other parametric resonance effects – see Appendix B of Ref. (5). Intuitively the reason is that larger λ 's require larger $c_{\mathcal{R}}$'s, see Eq. (31), diminishing therefore h_f given by Eq. (29), which sets the amplitude of the very first oscillations.

Nonetheless the standard perturbative approach to the inflaton decay provides a very efficient decay rate. Namely, at the SUSY vacuum v_H^c and \tilde{v}_H^c acquire the v.e.vs shown in Eq. (9) giving rise to the masses of the (canonically normalized) inflaton $\hat{\delta}h = (h - 2M_{\text{PS}}) / J_0$ and RH neutrinos, $\tilde{\nu}_i^c$, which are given, respectively, by

$$(a) \ m_I = \sqrt{2} \frac{\lambda M_{\text{PS}}}{\langle J \rangle f_0} \quad \text{and} \quad (b) \ M_{i\tilde{\nu}^c} = 2 \frac{\lambda_{i\nu^c} M_{\text{PS}}^2}{M_S \sqrt{f_0}}, \quad (33)$$

where f_0 is defined below Eq. (25b) and $\tilde{f}_0 = f_0 + 24c_{\mathcal{R}}^2 m_{\text{PS}}^2 \simeq J_0^2$. Here, we assume the existence of a term similar to the second one inside \ln of Eq. (7a) for ν_i^c too.

For larger λ 's $\langle J \rangle = J(h = 2M_{\text{PS}})$ ranges from 3 to 90 and so m_I is kept independent of λ and almost constant at the level of 10^{13} GeV. Indeed, if we express $\hat{\delta}h$ as a function of δh through the relation

$$\frac{\hat{\delta}h}{\delta h} \simeq J_0 \quad \text{where} \quad J_0 = \sqrt{1 + \frac{3}{2} m_P^2 f_{,h}^2 (\langle h \rangle)} = \sqrt{1 + 24c_{\mathcal{R}}^2 m_{\text{PS}}^2} \quad (34)$$

we find

$$m_1 \simeq \frac{\sqrt{2}\lambda M_{\text{PS}}}{f_0 J_0} \simeq \frac{\lambda m_{\text{P}}}{2\sqrt{3}c_{\mathcal{R}}} \simeq \frac{10^{-4}m_{\text{P}}}{4.2\sqrt{3}} \simeq 3 \cdot 10^{13} \text{ GeV for } \lambda \gtrsim \frac{10^{-4}}{4.2\sqrt{6}m_{\text{PS}}} \simeq 1.3 \cdot 10^{-3} \quad (35)$$

where we make use of Eq. (31) – note that $f_0 \simeq 1$. The derivation of the (s)particle spectrum, listed in Table 2, at the SUSY vacuum of the model reveals (5) that perturbative decays of $\hat{\delta h}$ into these massive particles are kinematically forbidden and therefore, narrow parametric resonance (40) effects are absent. Also $\hat{\delta h}$ can not decay via renormalizable interaction terms to SM particles.

The inflaton can decay into a pair of $\hat{\nu}_i^{c'}$'s through the following lagrangian terms:

$$\mathcal{L}_{\text{I}\nu^c} = -\lambda_{i\nu^c} \frac{M_{\text{PS}}}{M_{\text{S}}} \frac{f_0}{J_0} \left(1 - 12c_{\mathcal{R}}m_{\text{PS}}^2\right) \hat{\delta h} \hat{\nu}_i^c \hat{\nu}_i^c + \text{h.c.} \quad (36)$$

From Eq. (36) we deduce that the decay of $\hat{\delta h}$ into $\hat{\nu}_i^c$ is induced by two lagrangian terms. The first one originates exclusively from the non-renormalizable term of Eq. (5) – as in the case of a similar model in Ref. (30). The second term is a higher order decay channel due to the SUGRA lagrangian – cf. Ref. (43). The interaction in Eq. (36) gives rise to the following decay width

$$\Gamma_{\text{I}\hat{\nu}^c} = \frac{c_{\text{I}\hat{\nu}^c}^2}{64\pi} m_1 \sqrt{1 - \frac{4M_{\text{PS}}^2}{m_1^2}} \quad \text{with} \quad c_{\text{I}\hat{\nu}^c} = \frac{M_{\text{PS}}}{M_{\text{PS}}} \frac{f_0^{3/2}}{J_0} \left(1 - 12c_{\mathcal{R}}m_{\text{PS}}^2\right), \quad (37)$$

where M_{PS} is the Majorana mass of the $\hat{\nu}_j^c$'s into which the inflaton can decay. The implementation – see Sec. 4.3 – of the seesaw mechanism for the derivation of the light-neutrinos masses, in conjunction with the G_{PS} prediction $m_{3\text{D}} \simeq m_t$ and our assumption that $m_{1\text{D}} < m_{2\text{D}} \ll m_{3\text{D}}$ – see Sec. 5.1 – results to $2M_{3\hat{\nu}^c} > m_1$. Therefore, the kinematically allowed decay channels of $\hat{\delta h}$ are those into $\hat{\nu}_j^c$ with $j = 1$ and 2. Note that the decay of the inflaton to the heaviest of the $\hat{\nu}_j^c$'s ($\hat{\nu}_3^c$) is also disfavored by the \tilde{G} constraint – see below.

In addition, there are SUGRA-induced (43) – i.e., even without direct superpotential couplings – decay channels of the inflaton to the MSSM particles via non-renormalizable interaction terms. For a typical trilinear superpotential term of the form $W_y = yXYZ$, we obtain the effective interactions described by the langrangian part

$$\mathcal{L}_{\text{I}y} = 6yc_{\mathcal{R}} \frac{M_{\text{PS}}}{m_{\text{P}}^2} \frac{f_0^{3/2}}{2J_0} \hat{\delta h} \left(\hat{X} \hat{\psi}_Y \hat{\psi}_Z + \hat{Y} \hat{\psi}_X \hat{\psi}_Z + \hat{Z} \hat{\psi}_X \hat{\psi}_Y \right) + \text{h.c.}, \quad (38)$$

where y is a Yukawa coupling constant and ψ_X, ψ_Y and ψ_Z are the chiral fermions associated with the superfields X, Y and Z . Their scalar components are denoted with the superfield symbol. Taking into account the terms of Eq. (2) and the fact that the adopted SUSY GUT predicts YU for the 3rd generation at M_{PS} , we conclude that the interaction above gives rise to the following 3-body decay width

$$\Gamma_{\text{I}y} = \frac{14c_{\text{I}y}^2}{512\pi^3} m_1^3 \simeq \frac{3y_{33}^2}{64\pi^3} f_0^3 \left(\frac{m_1}{m_{\text{P}}} \right)^2 m_1 \quad \text{where} \quad c_{\text{I}y} = 6y_{33}c_{\mathcal{R}} \frac{M_{\text{PS}}}{m_{\text{P}}^2} \frac{f_0^{3/2}}{J_0}, \quad (39)$$

with $y_{33} \simeq (0.55 - 0.7)$ being the common Yukawa coupling constant of the third generation computed at the m_I scale, and summation is taken over color, weak and hypercharge degrees of freedom, in conjunction with the assumption that $m_I < 2M_{3\hat{\nu}^c}$.

Since the decay width of the produced $\hat{\nu}_j^c$ is much larger than Γ_I – see below – the reheating temperature, T_{rh} , is exclusively determined by the inflaton decay and is given by (44)

$$T_{\text{rh}} = \left(\frac{72}{5\pi^2 g_*} \right)^{1/4} \sqrt{\Gamma_I m_P} \quad \text{with} \quad \Gamma_I = \Gamma_{I1\hat{\nu}^c} + \Gamma_{I2\hat{\nu}^c} + \Gamma_{Iy}, \quad (40)$$

where g_* counts the effective number of relativistic degrees of freedom at temperature T_{rh} . For the MSSM spectrum plus the particle content of the superfields P and \bar{P} we find $g_* \simeq 228.75 + 4(1 + 7/8) = 236.25$.

4.2 LEPTON-NUMBER AND GRAVITINO ABUNDANCES

If $T_{\text{rh}} \ll M_{I\hat{\nu}^c}$, the out-of-equilibrium condition (2) for the implementation of nTL is automatically satisfied. Subsequently $\hat{\nu}_i^c$ decay into H_u and L_i^* via the tree-level couplings derived from the second term in the RHS of Eq. (2). Interference between tree-level and one-loop diagrams generates a lepton-number asymmetry (per $\hat{\nu}_j^c$ decay) ε_j (2), when CP conservation is violated. The resulting lepton-number asymmetry after reheating can be partially converted through sphaleron effects into baryon-number asymmetry. In particular, the B yield can be computed as

$$(a) \ Y_B = -0.35Y_L \quad \text{with} \quad (b) \ Y_L = 2 \frac{5}{4} \frac{T_{\text{rh}}}{m_I} \sum_{j=1}^2 \frac{\Gamma_{Ij\hat{\nu}^c}}{\Gamma_I} \varepsilon_j. \quad (41)$$

The numerical factor in the RHS of Eq. (41a) comes from the sphaleron effects, whereas the one (5/4) in the RHS of Eq. (41b) is due to the slightly different calculation (44) of T_{rh} – cf. Ref. (1). In the major part of our allowed parameter space – see Sec. 5.2 – $\Gamma_I \simeq \Gamma_{Iy}$ and so the involved branching ratio of the produced $\hat{\nu}_i^c$ is given by

$$\frac{\Gamma_{I1\hat{\nu}^c} + \Gamma_{I2\hat{\nu}^c}}{\Gamma_I} \simeq \frac{\Gamma_{I2\hat{\nu}^c}}{\Gamma_{Iy}} = \frac{\pi^2 (1 - 12c_{\mathcal{R}} m_{\text{PS}}^2)^2}{72c_{\mathcal{R}}^2 y_{33}^2 m_{\text{PS}}^4} \frac{M_{2\hat{\nu}^c}^2}{m_I^2}. \quad (42)$$

For $M_{2\hat{\nu}^c} \simeq (10^{11} - 10^{12})$ GeV the ratio above takes adequately large values so that Y_L is sizable. Therefore, the presence of more than one inflaton decay channels does not invalidate the scenario of nTL.

It is worth emphasizing, however, that if $M_{1\nu^c} \lesssim 10T_{\text{rh}}$, part of the Y_L can be washed out due to $\hat{\nu}_1^c$ mediated inverse decays and $\Delta L = 1$ scatterings – this possibility is analyzed in Ref. (27). Trying to avoid the relevant computational complications we limit ourselves to cases with $M_{1\hat{\nu}^c} \gtrsim 10T_{\text{rh}}$, so as any washout of the non-thermally produced Y_L is evaded. On the other hand, Y_L is not erased by the $\Delta L = 2$ scattering processes (45) at all temperatures T with $100 \text{ GeV} \lesssim T \lesssim T_{\text{rh}}$ since Y_L is automatically protected by SUSY (46) for $10^7 \text{ GeV} \lesssim T \lesssim T_{\text{rh}}$ and for $T \lesssim 10^7 \text{ GeV}$ these processes are well out of equilibrium provided that that mass of the heaviest light neutrino is 10 eV. This constraint, however, is overshadowed by a more stringent one induced by WMAP7 data (16) – see Sec. 5.1.

The required for successful nTL T_{rh} must be compatible with constraints on the \tilde{G} abundance, $Y_{\tilde{G}}$, at the onset of *nucleosynthesis* (BBN). This is estimated to be (19):

$$Y_{\tilde{G}} \simeq c_{\tilde{G}} T_{\text{rh}} \quad \text{with} \quad c_{\tilde{G}} = 1.9 \cdot 10^{-22} / \text{GeV}, \quad (43)$$

where we assume that \tilde{G} is much heavier than the gauginos. Let us note that non-thermal \tilde{G} production within SUGRA is (43) also possible. However, we here prefer to adopt the conservative approach based on the estimation of $Y_{\tilde{G}}$ via Eq. (43) since the latter \tilde{G} production depends on the mechanism of SUSY breaking.

Both Eqs. (41) and (43) yield the correct values of the B and \tilde{G} abundances provided that no entropy production occurs for $T < T_{\text{rh}}$. This fact can be easily achieved within our setting. The mass spectrum of the P - \bar{P} system is comprised by axion and saxion $P_- = (\bar{P} - P)/\sqrt{2}$, axino $\psi_- = (\psi_{\bar{P}} - \psi_P)/\sqrt{2}$, a higgs, $P_+ = (\bar{P} + P)/\sqrt{2}$, and a higgsino, $\psi_+ = (\psi_{\bar{P}} + \psi_P)/\sqrt{2}$, with mass of order 1 TeV and ψ denoting a Weyl spinor. The higgs and higgsinos can decay to lighter higgs and higgsinos before domination (36). Regarding the saxion, P_- , we can assume that its decay mode to axions is suppressed (w.r.t the ones to gluons, higgses and higgsinos (47; 48)) and the initial amplitude of its oscillations is equal to $f_a \simeq 10^{12}$ GeV. Under these circumstances, it can (47) decay before domination too, and evades (48) the constraints from the effective number of neutrinos for the f_a 's and T_{rh} 's encountered in our model. As a consequence of its relatively large decay temperature, the LSPs produced by the saxion decay are likely to be thermalized and therefore, no upper bound on the saxion abundance is (48) to be imposed. Finally, axino can not play the role of LSP due to its large expected mass and the relatively high T_{rh} 's encountered in our set-up which result to a large *Cold Dark Matter* (CDM) abundance. Nonetheless, it may enhance non-thermally the abundance of a higgsino-like neutralino-LSP, rendering it a successful CDM candidate.

4.3 LEPTON-NUMBER ASYMMETRY AND NEUTRINO MASSES

As mentioned above, the decay of $\hat{\nu}_2^c$ and $\hat{\nu}_1^c$, emerging from the \hat{h} decay, can generate a lepton asymmetry, ε_i (with $i = 1, 2$) caused by the interference between the tree and one-loop decay diagrams, provided that a CP-violation occurs in h_{Nij} 's. The produced ε_i can be expressed in terms of the Dirac mass matrix of ν_i , m_D , defined in a basis (called ν_i^c -basis henceforth) where ν_i^c are mass eigenstates, as follows:

$$\varepsilon_i = \sum_{j \neq i} \frac{\text{Im} \left[(m_D^\dagger m_D)_{ij}^2 \right]}{8\pi \langle H_u \rangle^2 (m_D^\dagger m_D)_{ii}} \left(F_S(x_{ij}, y_i, y_j) + F_V(x_{ij}) \right), \quad (44a)$$

where we take $\langle H_u \rangle \simeq 174$ GeV, for large $\tan \beta$ and

$$x_{ij} := \frac{M_{j\hat{\nu}^c}}{M_{i\hat{\nu}^c}} \quad \text{and} \quad y_i := \frac{\Gamma_{i\nu^c}}{M_{i\hat{\nu}^c}} = \frac{(m_D^\dagger m_D)_{ii}}{8\pi \langle H_u \rangle^2} \quad (44b)$$

(with $i, j = 1, 2, 3$). Also F_V and F_S represent, respectively, the contributions from vertex and self-energy diagrams which in SUSY theories read (49)

$$F_V(x) = -x \ln(1 + x^{-2}) \quad \text{and} \quad F_S(x, y, z) = \frac{-2x(x^2 - 1)}{(x^2 - 1)^2 + (x^2 z - y)^2}. \quad (44c)$$

Note that for strongly hierarchical $M_{\widehat{\nu}^c}$'s with $x_{ij} \gg 1$ and $x_{ij} \gg y_i, y_j$, we obtain the well-known approximate result (26; 27)

$$F_V + F_S \simeq -3/x_{ij}^2. \quad (45)$$

The involved in Eq. (44a) m_D can be diagonalized if we define a basis – called *weak basis* henceforth – in which the lepton Yukawa couplings and the $SU(2)_L$ interactions are diagonal in the space of generations. In particular we have

$$U^\dagger m_D U^{c\dagger} = d_D = \text{diag}(m_{1D}, m_{2D}, m_{3D}), \quad (46)$$

where U and U^c are 3×3 unitary matrices which relate L_i and ν_i^c (in the ν_i^c -basis) with the ones L'_i and $\nu_i^{c'}$ in the weak basis as follows:

$$L' = LU \quad \text{and} \quad \nu^{c'} = U^c \nu^c. \quad (47)$$

Here, we write LH lepton superfields, i.e. $SU(2)_L$ doublet leptons, as row 3-vectors in family space and RH anti-lepton superfields, i.e. $SU(2)_L$ singlet anti-leptons, as column 3-vectors. Consequently, the combination $m_D^\dagger m_D$ appeared in Eq. (44a) turns out to be a function just of d_D and U^c . Namely,

$$m_D^\dagger m_D = U^{c\dagger} d_D^\dagger d_D U^c. \quad (48)$$

The connection of the nTL scenario with the low energy neutrino data can be achieved through the seesaw formula, which gives the light-neutrino mass matrix m_ν in terms of m_{iD} and $M_{i\widehat{\nu}^c}$. Working in the ν_i^c -basis, we have

$$m_\nu = -m_D d_{\nu^c}^{-1} m_D^T, \quad \text{where} \quad d_{\nu^c} = \text{diag}(M_{1\widehat{\nu}^c}, M_{2\widehat{\nu}^c}, M_{3\widehat{\nu}^c}) \quad (49)$$

with $M_{1\widehat{\nu}^c} \leq M_{2\widehat{\nu}^c} \leq M_{3\widehat{\nu}^c}$ real and positive. Solving Eq. (46) w.r.t m_D and inserting the resulting expression in Eq. (49) we extract the mass matrix

$$\bar{m}_\nu = U^\dagger m_\nu U^* = -d_D U^c d_{\nu^c}^{-1} U^{cT} d_D, \quad (50)$$

which can be diagonalized by the unitary PMNS matrix satisfying

$$\bar{m}_\nu = U_\nu^* \text{diag}(m_{1\nu}, m_{2\nu}, m_{3\nu}) U_\nu^\dagger \quad (51)$$

and parameterized as follows:

$$U_\nu = \begin{pmatrix} c_{12}c_{13} & s_{12}c_{13} & s_{13}e^{-i\delta} \\ -c_{23}s_{12} - s_{23}c_{12}s_{13}e^{i\delta} & c_{23}c_{12} - s_{23}s_{12}s_{13}e^{i\delta} & s_{23}c_{13} \\ s_{23}s_{12} - c_{23}c_{12}s_{13}e^{i\delta} & -s_{23}c_{12} - c_{23}s_{12}s_{13}e^{i\delta} & c_{23}c_{13} \end{pmatrix} \cdot \begin{pmatrix} e^{-i\varphi_1/2} & 0 & 0 \\ 0 & e^{-i\varphi_2/2} & 0 \\ 0 & 0 & 1 \end{pmatrix}, \quad (52)$$

with $c_{ij} := \cos\theta_{ij}$, $s_{ij} := \sin\theta_{ij}$, δ the CP-violating Dirac phase and φ_1 and φ_2 the two CP-violating Majorana phases.

Following a bottom-up approach, along the lines of Ref. (26–28), we can find \bar{m}_ν via Eq. (51) using as input parameters the low energy neutrino observables, the CP violating phases and

adopting the normal or inverted hierarchical scheme of neutrino masses. Taking also m_{iD} as input parameters we can construct the complex symmetric matrix

$$W = -d_D^{-1} \bar{m}_\nu d_D^{-1} = U^c d_{\nu^c} U^{c\top} \quad (53)$$

– see Eq. (50) – from which we can extract d_{ν^c} as follows:

$$d_{\nu^c}^{-2} = U^{c\top} W W^\dagger U^c. \quad (54)$$

Note that $W W^\dagger$ is a 3×3 complex, hermitian matrix and can be diagonalized following the algorithm described in Ref. (50). Having determined the elements of U^c and the $M_{i\nu^c}$'s we can compute m_D through Eq. (48) and the ε_i 's through Eq. (44a).

5. CONSTRAINING THE MODEL PARAMETERS

We exhibit the constraints that we impose on our cosmological set-up in Sec. 5.1, and delineate the allowed parameter space of our model in Sec. 5.2.

5.1 IMPOSED CONSTRAINTS

The parameters of our model can be restricted once we impose the following requirements:

1. According to the inflationary paradigm, the horizon and flatness problems of the standard Big Bang cosmology can be successfully resolved provided that the number of e-foldings, \hat{N}_* , that the scale $k_* = 0.002/\text{Mpc}$ suffers during nMHI takes a certain value, which depends on the details of the cosmological model. Employing standard methods (51), we can easily derive the required \hat{N}_* for our model, consistently with the fact that the $P - \bar{P}$ system remains subdominant during the post-inflationary era. Namely we obtain

$$\hat{N}_* \simeq 22.5 + 2 \ln \frac{V_{\text{HI}}(h_*)^{1/4}}{1 \text{ GeV}} - \frac{4}{3} \ln \frac{V_{\text{HI}}(h_f)^{1/4}}{1 \text{ GeV}} + \frac{1}{3} \ln \frac{T_{\text{rh}}}{1 \text{ GeV}} + \frac{1}{2} \ln \frac{f(h_f)}{f(h_*)}. \quad (55)$$

2. The inflationary observables derived in Sec. 3.2 are to be consistent with the fitting (16) of the WMAP7, BAO and H_0 data. As usual, we adopt the central value of $\Delta_{\mathcal{R}}$, whereas we allow the remaining quantities to vary within the 95% confidence level (c.l.) ranges. Namely,

$$(a) \Delta_{\mathcal{R}} \simeq 4.93 \cdot 10^{-5}, (b) n_s = 0.968 \pm 0.024, (c) -0.062 \leq a_s \leq 0.018 \text{ and } (d) r < 0.24 \quad (56)$$

3. The scale M_{PS} can be determined by requiring that the v.e.vs of the Higgs fields take the values dictated by the unification of the gauge couplings within the MSSM. As we now recognize – cf. Ref. (5) – the unification scale $M_{\text{GUT}} \simeq 2 \cdot 10^{16} \text{ GeV}$ is to be identified with the *lowest* mass scale of the model in the SUSY vacuum, Eq. (9), in order to avoid any extra contribution to the running of the MSSM gauge couplings, i.e.,

$$(a) \frac{g M_{\text{PS}}}{\sqrt{f_0}} = M_{\text{GUT}} \Rightarrow m_{\text{PS}} = \frac{1}{2\sqrt{2c_{\mathcal{R}}^{\text{max}} - c_{\mathcal{R}}}} \text{ with } (b) c_{\mathcal{R}}^{\text{max}} = \frac{g^2 m_{\text{P}}^2}{8M_{\text{GUT}}^2} \quad (57)$$

The requirement $2c_{\mathcal{R}}^{\text{max}} - c_{\mathcal{R}} > 0$ sets an upper bound $c_{\mathcal{R}} < 2c_{\mathcal{R}}^{\text{max}} \simeq 1.8 \cdot 10^3$, which however can be significantly lowered if we combine Eqs. (55) and (28) – see Sec. 5.2.1.

4. For the realization of nMHI, we assume that $c_{\mathcal{R}}$ takes relatively large values – see e.g. Eq. (17). This assumption may (52; 53) jeopardize the validity of the classical approximation, on which the analysis of the inflationary behavior is based. To avoid this inconsistency – which is rather questionable (11; 54) though – we have to check the hierarchy between the ultraviolet cut-off, $\Lambda = m_{\text{P}}/c_{\mathcal{R}}$, of the effective theory and the inflationary scale, which is represented by $\hat{V}_{\text{HI}}(h_*)^{1/4}$ or, less restrictively, by the corresponding Hubble parameter, $\hat{H}_* = \hat{V}_{\text{HI}}(h_*)^{1/2}/\sqrt{3}m_{\text{P}}$. In particular, the validity of the effective theory implies (52; 53)

$$(a) \hat{V}_{\text{HI}}(h_*)^{1/4} \leq \Lambda \text{ or } (b) \hat{H}_* \leq \Lambda \text{ for } (c) c_{\mathcal{R}} \geq 1. \quad (58)$$

5. As discussed in Sec. 4.2, to avoid any erasure of the produced Y_L and to ensure that the inflaton decay to $\hat{\nu}_2$ is kinematically allowed we have to bound $M_{1\hat{\nu}^c}$ and $M_{2\hat{\nu}^c}$ respectively as follows:

$$(a) M_{1\hat{\nu}^c} \gtrsim 10T_{\text{rh}} \text{ and } (b) m_1 \geq 2M_{2\hat{\nu}^c} \Rightarrow M_{2\hat{\nu}^c} \lesssim \frac{\lambda m_{\text{P}}}{4\sqrt{3}c_{\mathcal{R}}} \simeq 1.5 \cdot 10^{13} \text{ GeV}, \quad (59)$$

where we make use of Eq. (35). Recall that we impose also the restriction $\lambda \geq 0.001$ which allows us to ignore effects of instant preheating (5; 42).

6. As discussed below Eq. (2), the adopted GUT predicts YU at M_{GUT} . Assuming negligible running of $m_{3\text{D}}$ from M_{GUT} until the scale of nTL, Λ_L , which is taken to be $\Lambda_L = m_1$, we end up with the requirement:

$$m_{3\text{D}}(m_1) = m_t(m_1) \simeq (100 - 120) \text{ GeV}. \quad (60)$$

where m_t is the top quark mass and the numerical values correspond to $y_{33}(m_1) = (0.55 - 0.7)$ – cf. Ref. (55) – found (32; 56) working in the context of several MSSM versions with $\tan \beta \simeq 50$ and taking into account the SUSY threshold corrections. As regards the lighter generation, we limit ourselves in imposing just a mild hierarchy between $m_{1\text{D}}$ and $m_{2\text{D}}$, i.e., $m_{1\text{D}} < m_{2\text{D}} \ll m_{3\text{D}}$ since it is not possible to achieve a simultaneous fulfilment of all the residual constraints if we impose relations similar to Eq. (60) – cf. Ref. (25–27).

7. From the solar, atmospheric, accelerator and reactor neutrino experiments we take into account the inputs listed in Table 3 on the neutrino mass-squared differences Δm_{21}^2 and Δm_{31}^2 , on the mixing angles θ_{ij} and on the CP-violating Dirac phase, δ for normal [inverted] neutrino mass hierarchy (23) – see also Ref. (24). In particular, $m_{i\nu}$'s can be determined via the relations:

$$m_{2\nu} = \sqrt{m_{1\nu}^2 + \Delta m_{21}^2} \text{ and } \begin{cases} m_{3\nu} = \sqrt{m_{1\nu}^2 + \Delta m_{31}^2}, & \text{for normally ordered (NO) } m_{\nu}\text{'s} \\ \text{or} \\ m_{1\nu} = \sqrt{m_{3\nu}^2 + |\Delta m_{31}^2|}, & \text{for invertedly ordered (IO) } m_{\nu}\text{'s} \end{cases} \quad (61)$$

The sum of $m_{i\nu}$'s can be bounded from above by the WMAP7 data (16)

$$\sum_i m_{i\nu} \leq 0.58 \text{ eV} \quad (62)$$

at 95% c.l. This is more restrictive than the 95% c.l. upper bound arising from the effective electron neutrino mass in β -decay (57):

$$m_{\beta} := \left| \sum_i U_{1i\nu}^2 m_{i\nu} \right| \leq 2.3 \text{ eV}. \quad (63)$$

PARAMETER	BEST FIT $\pm 1\sigma$	
	NORMAL	INVERTED
	HIERARCHY	
$\Delta m_{21}^2 / 10^{-3} \text{eV}^2$	7.62 ± 0.19	
$\Delta m_{31}^2 / 10^{-3} \text{eV}^2$	$2.53^{+0.08}_{-0.10}$	$-2.4^{+0.10}_{-0.07}$
$\sin^2 \theta_{12}$	$0.320^{+0.015}_{-0.017}$	
$\sin^2 \theta_{13}$	$0.026^{+0.003}_{-0.004}$	$0.027^{+0.003}_{-0.004}$
$\sin^2 \theta_{23}$	$0.49^{+0.08}_{-0.05}$	$0.53^{+0.05}_{-0.07}$
δ / π	$0.83^{+0.54}_{-0.64}$	0.07

TABLE 3. Low energy experimental neutrino data for normal or inverted hierarchical neutrino masses. In the second case the full range $(0 - 2\pi)$ is allowed at 1σ for the phase δ .

However, in the future, the KATRIN experiment (58) expects to reach the sensitivity of $m_\beta \simeq 0.2 \text{ eV}$ at 90% c.l.

8. The interpretation of BAU through nTL dictates (16) at 95% c.l.

$$Y_B = (8.74 \pm 0.42) \cdot 10^{-11} \Rightarrow 8.32 \leq 10^{11} Y_B \leq 9.16. \quad (64)$$

9. In order to avoid spoiling the success of the BBN, an upper bound on $Y_{\tilde{G}}$ is to be imposed depending on the \tilde{G} mass, $m_{\tilde{G}}$, and the dominant \tilde{G} decay mode. For the conservative case where \tilde{G} decays with a tiny hadronic branching ratio, we have (19)

$$Y_{\tilde{G}} \lesssim \begin{cases} 10^{-14} \\ 10^{-13} \\ 10^{-12} \end{cases} \text{ for } m_{\tilde{G}} \simeq \begin{cases} 0.69 \text{ TeV} \\ 10.6 \text{ TeV} \\ 13.5 \text{ TeV} \end{cases} \quad (65)$$

As we see below, this bound is achievable within our model only for $m_{\tilde{G}} \gtrsim 10 \text{ TeV}$. Taking into account that the soft masses of the scalars are not necessarily equal to $m_{\tilde{G}}$, we do not consider such a restriction as a very severe tuning of the SUSY parameter space. Using Eq. (43) the bounds on $Y_{\tilde{G}}$ can be translated into bounds on T_{rh} . Specifically we take $T_{\text{rh}} \simeq (0.53 - 5.3) \cdot 10^8 \text{ GeV}$ [$T_{\text{rh}} \simeq (0.53 - 5.3) \cdot 10^9 \text{ GeV}$] for $Y_{\tilde{G}} \simeq (0.1 - 1) \cdot 10^{-13}$ [$Y_{\tilde{G}} \simeq (0.1 - 1) \cdot 10^{-12}$].

Let us, finally, comment on the axion isocurvature perturbations generated in our model. Indeed, since the PQ symmetry is broken during nMHI, the axion acquires quantum fluctuations as all the almost massless degrees of freedom. At the QCD phase transition, these fluctuations turn into isocurvature perturbations in the axion energy density, which means that the partial curvature perturbation in axions is different than the one in photons. The results of WMAP put stringent bounds on the possible CDM isocurvature perturbation.

Namely, taking into account the WMAP7, BAO and H_0 data on the parameter α_0 we find the following bound for the amplitude of the CDM isocurvature perturbation

$$|\mathcal{S}_c| = \Delta_{\mathcal{R}} \sqrt{\frac{\alpha_0}{1 - \alpha_0}} \lesssim 1.5 \cdot 10^{-5} \text{ at } 95\% \text{ c.l.} \quad (66)$$

On the other, $|\mathcal{S}_c|$ due to axion, can be estimated by

$$|\mathcal{S}_c| = \frac{\Omega_a}{\Omega_c} \frac{\hat{H}_{\text{HI}}}{\pi |\theta_1| \hat{\phi}_{P*}} \text{ with } \frac{\Omega_a}{\Omega_c} \simeq \theta_1^2 \left(\frac{f_a}{1.56 \cdot 10^{11} \text{ GeV}} \right)^{1.175} \quad (67)$$

where Ω_a [Ω_c] is the axion [CDM] density parameter, $\hat{\phi}_{P*} \sim 10^{16} \text{ GeV}$ (36) denotes the field value of the PQ scalar when the cosmological scales exit the horizon and θ_1 is the initial misalignment angle which lies (36) in the interval $[-\pi/6, \pi/6]$. Satisfying Eq. (66) requires $|\theta_1| \lesssim \pi/70$ which is a rather low but not unacceptable value. Therefore, a large axion contribution to CDM is disfavored within our model.

5.2 NUMERICAL RESULTS

As can be seen from the relevant expressions in Secs. 2 and 4, our cosmological set-up depends on the parameters:

$$\lambda, \lambda_H, \lambda_{\bar{H}}, k_S, g, y_{33}, m_{\ell\nu}, m_{iD}, \varphi_1 \text{ and } \varphi_2,$$

where $m_{\ell\nu}$ is the low scale mass of the lightest of ν_i 's and can be identified with $m_{1\nu}$ [$m_{3\nu}$] for NO [IO] neutrino mass spectrum. Recall that we determine M_{PS} via Eq. (57) with $g = 0.7$. We do not consider $c_{\mathcal{R}}$ and $\lambda_{i\nu^c}$ as independent parameters since $c_{\mathcal{R}}$ is related to m via Eq. (31) while $\lambda_{i\nu^c}$ can be derived from the last six parameters above which affect exclusively the Y_L calculation and can be constrained through the requirements 5 - 9 of Sec. 5.1. Note that the $\lambda_{i\nu^c}$'s can be replaced by $M_{i\nu^c}$'s given in Eq. (33b) keeping in mind that perturbativity requires $\lambda_{i\nu^c} \leq \sqrt{4\pi}$ or $M_{i\nu^c} \leq 10^{16} \text{ GeV}$. Note that if we replace M_S with m_P in Eq. (5), we obtain a tighter bound, i.e., $M_{i\nu^c} \leq 2.3 \cdot 10^{15} \text{ GeV}$. Our results are essentially independent of $\lambda_H, \lambda_{\bar{H}}$ and k_S , provided that we choose some relatively large values for these so as m_{u-}^2, m_{d-}^2 and m_S^2 in Table 2 are positive for $\lambda < 1$. We therefore set $\lambda_H = \lambda_{\bar{H}} = 0.5$ and $k_S = 1$ throughout our calculation. Finally T_{rh} can be calculated self-consistently in our model as a function of $m_t, M_{2\nu^c} \gg M_{1\nu^c}$ and the unified Yukawa coupling constant y_{33} – see Sec. 4.1 – for which we take $y_{33} = 0.6$.

Summarizing, we set throughout our calculation:

$$k_S = 1, \lambda_H = \lambda_{\bar{H}} = 0.5, g = 0.7 \text{ and } y_{33} = 0.6. \quad (68)$$

The selected values for the above quantities give us a wide and natural allowed region for the remaining fundamental parameters of our model, as we show below concentrating separately in the inflationary period (Sec. 5.2.1) and in the stage of nTL (Sec. 5.2.2).

5.2.1 The Inflationary Stage

In this part of our numerical code, we use as input parameters $h_*, m_{2D} \gg m_{1D}$ and $c_{\mathcal{R}}$. For every chosen $c_{\mathcal{R}} \geq 1$ and m_{2D} , we restrict λ and h_* so that the conditions Eq. (55) and (56a) are satisfied. In our numerical calculations, we use the complete formulas for the slow-roll

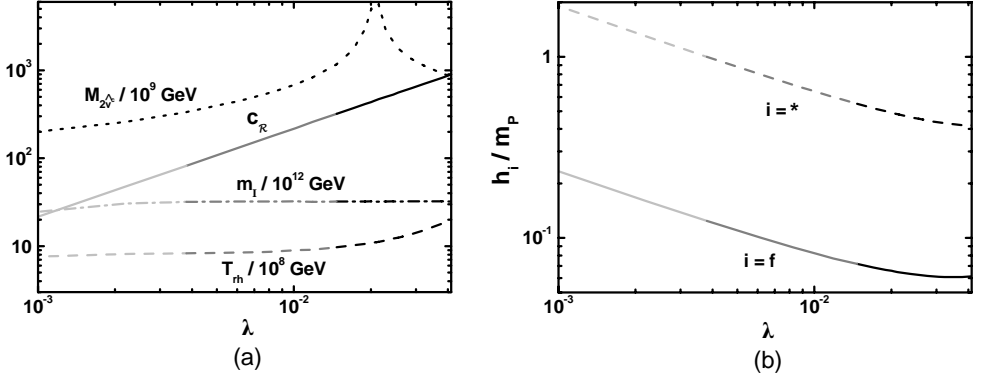


FIGURE 1. The allowed (by all the imposed constraints) values of $c_{\mathcal{R}}$ (solid line), T_{th} – given by Eq. (40) – (dashed line), m_1 (dot-dashed line) and $M_{2\nu^c}$ (dotted line) [h_f (solid line) and h_* (dashed line)] versus λ (a) [(b)] for $k_S = 1$, $\lambda_H = \lambda_{\bar{H}} = 0.5$ and $y_{33} = 0.6$. The light gray and gray segments denote values of the various quantities satisfying Eq. (58a) too, whereas along the light gray segments we obtain $h_* \geq m_P$.

parameters and $\Delta_{\mathcal{R}}$ in Eqs. (25a), (25b) and (30) and not the approximate relations listed in Sec. 3.2 for the sake of presentation. Our results are displayed in Fig. 1, where we draw the allowed values of $c_{\mathcal{R}}$ (solid line), T_{th} (dashed line), the inflaton mass, m_1 (dot-dashed line) and $M_{2\nu^c}$ (dotted line) – see Sec. 4.1 – [h_f (solid line) and h_* (dashed line)] versus λ (a) [(b)] for the m_{2D} 's required from Eq. (64) and for the parameters adopted along the black dashed line of Fig. 2 – see Sec. 5.2.2. The required via Eq. (55) \hat{N}_* remains almost constant and close to 54.5.

The lower bound of the depicted lines comes from the saturation of the Eq. (58c). The constraint of Eq. (58b) is satisfied along the various curves whereas Eq. (58a) is valid only along the gray and light gray segments of these. Along the light gray segments, though, we obtain $h_* \geq m_P$. The latter regions of parameter space are not necessarily excluded, since the energy density of the inflaton remains sub-Planckian and so, corrections from quantum gravity can still be assumed to be small. As $c_{\mathcal{R}}$ increases beyond 906, f_0 becomes much larger than 1, \hat{N}_* derived by Eq. (28) starts decreasing and therefore, nMHI fails to fulfil Eq. (55). This can be understood by the observation that \hat{N}_* , approximated fairly by Eq. (29), becomes monotonically decreasing function of $c_{\mathcal{R}}$ for $c_{\mathcal{R}} > c_{\mathcal{R}}^{\text{max}}$ where $c_{\mathcal{R}}^{\text{max}}$ can be found by the condition

$$\frac{d\hat{N}_*}{dc_{\mathcal{R}}} \simeq \frac{3h_*^2}{4m_P^2} \frac{(c_{\mathcal{R}}^{\text{max}} - c_{\mathcal{R}})}{c_{\mathcal{R}}^{\text{max}}} = 0 \Rightarrow c_{\mathcal{R}} \simeq c_{\mathcal{R}}^{\text{max}}, \quad (69)$$

where $c_{\mathcal{R}}^{\text{max}}$ is defined in Eq. (57b) and Eq. (57a) is also taken into account. As a consequence, the embedding of nMHI in a SUSY GUT provides us with a clear upper bound of $c_{\mathcal{R}}$. All in all, we obtain

$$0.001 \lesssim \lambda \lesssim 0.042 \text{ and } 1 \lesssim c_{\mathcal{R}} \lesssim 907 \text{ for } \hat{N}_* \simeq 54.5 \quad (70)$$

When $c_{\mathcal{R}}$ ranges within its allowed region, we take $M_{\text{PS}} \simeq (2.87 - 4) \cdot 10^{16}$ GeV.

From Fig. 1-(a), we can verify our analytical estimation in Eq. (31) according to which λ is proportional to $c_{\mathcal{R}}$. On the other hand, the variation of h_f and h_* as a function of $c_{\mathcal{R}}$ – drawn in Fig. 1-(b) – is consistent with Eqs. (27) and (29). Letting λ or $c_{\mathcal{R}}$ vary within its allowed

region in Eq. (70), we obtain

$$n_s \simeq 0.964, \quad \alpha_s \simeq -6.35 \cdot 10^{-4} \quad \text{and} \quad r \simeq 3.6 \cdot 10^{-3}. \quad (71)$$

Clearly, the predicted α_s and r lie within the allowed ranges given in Eq. (56b) and Eq. (56c) respectively, whereas n_s turns out to be impressively close to its central observationally favored value – see Eq. (56a) and cf. Ref. (12).

From Fig. 1-(a) we can conclude that m_1 is kept independent of λ and almost constant at the level of 10^{13} GeV, as anticipated in Eq. (35). From the same plot we also remark that for $\lambda \lesssim 0.03$, T_{rh} remains almost constant since $\Gamma_{1\gamma}$ dominates over $\Gamma_{12\hat{\nu}^c}$ and $f_0^3 \simeq 1$ – see Eq. (39). For $\lambda \gtrsim 0.03$, $f_0^3 \simeq 1 + 12c_{\mathcal{R}}m_{\text{PS}}^2$ starts to deviate from unity and so, T_{rh} increases with $c_{\mathcal{R}}$ or λ as shown in Fig. 1. The required by Eq. (64) $M_{2\hat{\nu}^c}$ follows the behavior of the required m_{2D} – see Fig. 2-(a) of Sec. 5.2.2.

5.2.2 The Stage of non-Thermal Leptogenesis

In this part of our numerical program, for a given neutrino mass scheme, we take as input parameters: $m_{\ell\nu}, m_{iD}, \varphi_1, \varphi_2$ and the best-fit values of the neutrino parameters listed in Table 3. We then find the *renormalization group* (RG) evolved values of these parameters at the scale of nTL, Λ_L , which is taken to be $\Lambda_L = m_1$, integrating numerically the complete expressions of the RG equations – given in Ref. (29) – for $m_{i\nu}, \theta_{ij}, \delta, \varphi_1$ and φ_2 . In doing this, we consider the MSSM with $\tan\beta \simeq 50$, favored by the preliminary LHC results – see, e.g., Ref. (32; 56) – as an effective theory between Λ_L and a SUSY-breaking scale, $M_{\text{SUSY}} = 1.5$ TeV. Following the procedure described in Sec. 4.3, we evaluate $M_{i\hat{\nu}^c}$ at Λ_L . We do not consider the running of m_{iD} and $M_{i\hat{\nu}^c}$ and therefore, we give their values at Λ_L .

We start the exposition of our results arranging in Table 4 some representative values of the parameters leading to the correct BAU for $\lambda = 0.01$ and $c_{\mathcal{R}} = 220$ and normally hierarchical (cases A and B), degenerate (cases C, D and E) and invertedly hierarchical (cases F and G) m_ν 's. For comparison we display the B -yield with (Y_B) or without (Y_B^0) taking into account the RG effects. We observe that the two results are more or less close with each other. In all cases the current limit of Eq. (62) is safely met – the case D approaches it –, while m_β turns out to be well below the projected sensitivity of KATRIN (58). Shown are also the obtained T_{rh} 's, which are close to 10^9 GeV in all cases, and the corresponding $Y_{\tilde{G}}$'s, which are consistent with Eq. (65) for $m_{\tilde{G}} \gtrsim 11$ TeV.

From Table 4 we also remark that the achievement of Y_B within the range of Eq. (64) dictates a clear hierarchy between the $M_{i\hat{\nu}^c}$'s, which follows the imposed hierarchy in the sector of m_{iD} 's – see paragraph 6 of Sec. 5.1. This is expected since, in the limit of hierarchical m_{iD} 's, the $M_{i\hat{\nu}^c}$'s can be approximated by the following expressions (25; 26)

$$(M_{1\hat{\nu}^c}, M_{2\hat{\nu}^c}, M_{3\hat{\nu}^c}) \sim \begin{cases} \left(\frac{m_{1D}^2}{m_{2\nu}s_{12}^2}, \frac{2m_{2D}^2}{m_{3\nu}}, \frac{m_{3D}^2s_{12}^2}{2m_{1\nu}} \right) & \text{for NO } m_\nu\text{'s} \\ \left(\frac{m_{1D}^2}{\sqrt{|\Delta m_{31}|}}, \frac{2m_{2D}^2}{\sqrt{|\Delta m_{31}|}}, \frac{m_{3D}^2}{2m_{3\nu}} \right) & \text{for IO } m_\nu\text{'s} \end{cases} \quad (72a)$$

Indeed, we see e.g. that for fixed j , the $M_{j\hat{\nu}^c}$'s depends exclusively on the m_{jD} 's and $M_{3\hat{\nu}^c}$ increases when $m_{\ell\nu}$ decreases with fixed m_{3D} . As a consequence, satisfying Eq. (59a) pushes the m_{1D} 's well above the mass of the quark of the first generation. Similarly, the m_{2D} 's required by Eq. (64) turns out to be heavier than the quark of the second generation. Also, the required

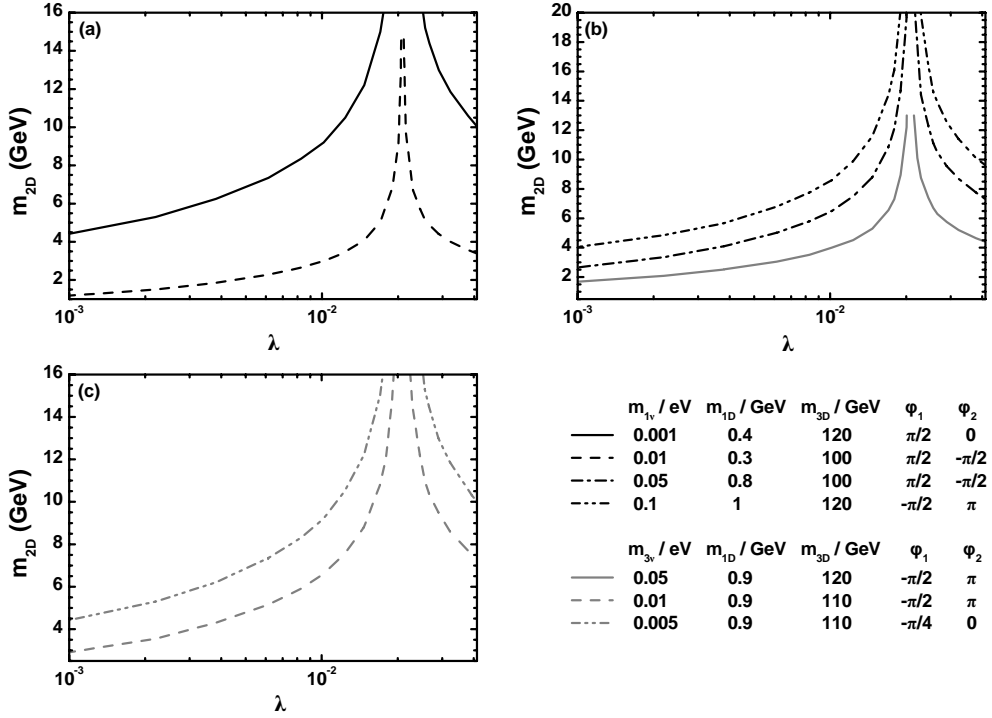
PARAMETERS	CASES						
	A	B	C	D	E	F	G
	NORMAL HIERARCHY		DEGENERATE MASSES			INVERTED HIERARCHY	
LOW SCALE PARAMETERS							
$m_{1\nu}/0.1\text{ eV}$	0.01	0.1	0.5	1.	0.7	0.5	0.49
$m_{2\nu}/0.1\text{ eV}$	0.088	0.13	0.5	1.	0.7	0.51	0.5
$m_{3\nu}/0.1\text{ eV}$	0.5	0.5	0.71	1.1	0.5	0.1	0.05
$\sum_i m_{i\nu}/0.1\text{ eV}$	0.6	0.74	1.7	3.1	1.9	1.1	1
$m_{\beta}/0.1\text{ eV}$	0.03	0.013	0.14	0.68	0.45	0.33	0.4
φ_1	$\pi/2$	$\pi/2$	$\pi/2$	$-\pi/2$	$-\pi/2$	$-\pi/2$	$-\pi/4$
φ_2	0	$-\pi/2$	$-\pi/2$	π	π	π	0
LEPTOGENESIS-SCALE PARAMETERS							
m_{1D}/GeV	0.4	0.3	0.8	1	0.9	0.9	0.9
m_{2D}/GeV	9.2	3	6.5	8.6	3.95	6.6	9.2
m_{3D}/GeV	120	100	100	120	120	110	110
$M_{1\tilde{\nu}^c}/10^{10}\text{ GeV}$	4.4	4.7	3.6	1.2	1.5	1.6	1.7
$M_{2\tilde{\nu}^c}/10^{12}\text{ GeV}$	2.7	0.6	0.65	1.5	0.9	1.5	2.8
$M_{3\tilde{\nu}^c}/10^{14}\text{ GeV}$	27	0.28	0.46	0.4	0.4	3.8	10
RESULTING B -YIELD							
$10^{11}Y_B^0$	8.75	8.9	8.6	8.63	8.9	9.	8.76
$10^{11}Y_B$	9.3	8.7	8.5	8.4	9.7	8.8	9.2
RESULTING T_{rh} AND $Y_{\tilde{G}}$							
$T_{\text{rh}}/10^9\text{ GeV}$	1.2	0.89	0.89	0.99	0.91	0.99	1.2
$10^{13}Y_{\tilde{G}}$	2.4	1.7	1.7	1.9	1.7	1.88	1.88

TABLE 4. Parameters yielding the correct BAU for various neutrino mass schemes for $\lambda = 0.01$ and $c_{\mathcal{R}} = 220$.

by seesaw $M_{3\tilde{\nu}^c}$'s are lower in the case of degenerate ν_i spectra and can be as low as $3 \cdot 10^{13} \text{ GeV}$ in sharp contrast to our findings in Ref. (5), where much larger $M_{3\tilde{\nu}^c}$'s are necessitated. An order of magnitude estimation for the derived ε_L 's can be achieved by (25; 26)

$$\varepsilon_2 \sim -\frac{3M_{2\tilde{\nu}^c}}{8\pi\langle H_u \rangle^2} \begin{cases} \left(\frac{m_{1\nu}}{s_{12}^2} \right) & \text{for NO } m_\nu\text{'s} \\ m_{3\nu} & \text{for IO } m_\nu\text{'s} \end{cases} \quad (72b)$$

which is rather accurate, especially in the case of IO m_ν 's.



$m_{1\nu}$ (eV)	λ (10^{-2})	m_{2D} (GeV)	$M_{1\nu^c}$ (10^{10} GeV)	$M_{2\nu^c}$ (10^{12} GeV)	$M_{3\nu^c}$ (10^{14} GeV)
0.001	0.1 – 1.8	5.5 – 17	4.7	1 – 9.8	32
	2.4 – 4.1	17 – 10	4.7	17 – 10	32
0.01	0.1 – 2	1.5 – 13	3.5 – 6	0.26 – 8.75	0.33 – 0.4
	2 – 4.1	15 – 3.4	6 – 5.3	11 – 0.84	0.42 – 0.34
0.05	0.1 – 2	3 – 28	3.5 – 4	2.1 – 11	0.5 – 0.6
	2.1 – 4.1	28 – 7.3	4 – 3.9	11 – 0.8	0.6 – 0.5
0.1	0.1 – 1.9	4 – 23	1.3	0.4 – 8	0.4 – 0.5
	2.2 – 4.1	23 – 9	1.3	10 – 2	0.5 – 0.4
$m_{3\nu}$ (eV)	λ (10^{-2})	m_{2D} (GeV)	$M_{1\nu^c}$ (10^{10} GeV)	$M_{2\nu^c}$ (10^{12} GeV)	$M_{3\nu^c}$ (10^{14} GeV)
0.05	0.1 – 2	2.1 – 12	1.5 – 1.6	0.28 – 7.8	0.48 – 0.56
	2.1 – 4.1	13 – 4.4	1.6	8.7 – 1.2	0.57 – 0.49
0.01	0.1 – 2	2.8 – 17	2.2	0.4 – 11	5.4 – 5.6
	2 – 4.1	17 – 7.3	2.2	11 – 2	5.6 – 5.4
0.005	0.1 – 1.8	5 – 17	1.8	0.7 – 10.1	12
	1.8 – 4.1	17.7 – 10	1.8	10.5 – 3.5	12

FIGURE 2. Contours on the $\lambda - m_{2D}$ plane, yielding the central Y_B in Eq. (64), consistently with the inflationary requirements, for $\lambda_H = \lambda_{\bar{H}} = 0.5$, $k_S = 1$ and $y_{33} = 0.6$ and various $(m_{\ell\nu}, m_{1D}, \phi_1, \phi_2)$'s indicated next to the graph (c) and NO [IO] $m_{i\nu}$'s (black [gray] lines). The corresponding ranges of $M_{i\nu^c}$'s are also shown in the table included.

To highlight further our conclusions inferred from Table 4, we can fix $m_{\ell\nu}$ ($m_{1\nu}$ for NO $m_{i\nu}$'s or $m_{3\nu}$ for IO $m_{i\nu}$'s) m_{1D} , m_{3D} , φ_1 and φ_2 to their values shown in this table and vary m_{2D} so that the central value of Eq. (64) is achieved. This is doable since, according Eq. (72a), variation of m_{2D} induces an exclusive variation to $M_{2\hat{\nu}^c}$ which, in turn, heavily influences ε_L – see Eqs. (44a) and (45) – and Y_L – see Eqs. (41) and (42). The resulting contours in the $\lambda - m_{2D}$ plane are presented in Fig. 2 – since the range of Eq. (64) is very narrow the possible variation of the drawn lines is negligible. The resulting $M_{j\hat{\nu}^c}$'s are displayed in the table included. The conventions adopted for the types and the color of the various lines are also described next to the graph (c) of Fig. 2. In particular, we use black [gray] lines for NO [IO] $m_{i\nu}$'s. The black dashed and the solid gray line terminate at the values of m_{2D} beyond which Eq. (64) is non fulfilled due to the violation of Eq. (59b).

In all cases, two disconnected allowed domains arise according to which of the two contributions in Eq. (36) dominates. The critical point $(\lambda_c, c_{\mathcal{R}c})$ is extracted from:

$$1 - 12c_{\mathcal{R}c}m_{\text{PS}}^2 = 0 \Rightarrow c_{\mathcal{R}c} = c_{\mathcal{R}}^{\text{max}}/2 \simeq 453 \text{ or } \lambda_c \simeq 10^{-4}c_{\mathcal{R}}^{\text{max}}/4.2 \simeq 0.021 \quad (73)$$

where we make use of Eq. (57) and Eq. (31) in the intermediate and the last step respectively. From Eqs. (40), (41) and (42) one can deduce that for $\lambda < \lambda_c$, T_{rh} remains almost constant; $\Gamma_{12\hat{\nu}^c}/\Gamma_I$ decreases as $c_{\mathcal{R}}$ increases and so the $M_{2\hat{\nu}^c}$'s, which satisfy Eq. (64), increase. On the contrary, for $\lambda > \lambda_c$, $\Gamma_{12\hat{\nu}^c}/\Gamma_I$ is independent of $c_{\mathcal{R}}$ but T_{rh} increases with $c_{\mathcal{R}}$ and so the fulfilling Eq. (64) $M_{2\hat{\nu}^c}$'s decrease.

Summarizing, we conclude that our scenario prefers the following ranges for the $M_{i\hat{\nu}^c}$'s:

$$1 \lesssim M_{1\hat{\nu}^c}/10^{10} \text{ GeV} \lesssim 6, \quad 0.6 \lesssim M_{2\hat{\nu}^c}/10^{12} \text{ GeV} \lesssim 20, \quad 0.3 \lesssim M_{3\hat{\nu}^c}/10^{14} \text{ GeV} \lesssim 30, \quad (74a)$$

while the m_{1D} and m_{2D} are restricted in the ranges:

$$0.3 \lesssim m_{1D}/\text{GeV} \lesssim 1, \quad 1.5 \lesssim m_{2D}/\text{GeV} \lesssim 20. \quad (74b)$$

6. CONCLUSIONS

We investigated the implementation of nTL within a realistic GUT, based on the PS gauge group. Leptogenesis follows a stage of nMHI driven by the radial component of the Higgs field, which leads to the spontaneous breaking of the PS gauge group to the SM one with the GUT breaking v.e.v identified with the SUSY GUT scale and without overproduction of monopoles. The model possesses also a resolution to the strong CP and the μ problems of the MSSM via a PQ symmetry which is broken during nMHI and afterwards. As a consequence the axion cannot be the dominant component of CDM, due to the present bounds on the axion isocurvature fluctuation. Moreover, we briefly discussed scenaria in which the potential axino and saxion overproduction problems can be avoided.

Inflation is followed by a reheating phase, during which the inflaton can decay into the lightest, $\hat{\nu}_1^c$, and the next-to-lightest, $\hat{\nu}_2^c$, RH neutrinos allowing, thereby for nTL to occur via the subsequent decay of $\hat{\nu}_1^c$ and $\hat{\nu}_2^c$. Although other decay channels to the SM particles via non-renormalizable interactions are also activated, we showed that the production of the required by the observations BAU can be reconciled with the observational constraints on the inflationary observables and the \tilde{G} abundance, provided that the (unstable) \tilde{G} masses are greater than 11 TeV. The required by the observations BAU can become consistent with the

present low energy neutrino data, the restriction on m_{3D} due to the PS gauge group and the imposed mild hierarchy between m_{1D} and m_{2D} . To this end, m_{1D} and m_{2D} turn out to be heavier than the ones of the corresponding quarks and lie in the ranges $(0.1 - 1)$ GeV and $(2 - 20)$ GeV while the obtained $M_{1\hat{\nu}^c}$, $M_{2\hat{\nu}^c}$ and $M_{3\hat{\nu}^c}$ are restricted to the values 10^{10} GeV, $(10^{11} - 10^{12})$ GeV and $(10^{13} - 10^{15})$ GeV respectively.

ACKNOWLEDGEMENTS

We would like to thank A.B. Lahanas, G. Lazarides and V.C. Spanos for valuable discussions.

REFERENCES

- [1] Hamaguchi K. *Phd Thesis*, hep-ph/0212305.
- [2] Buchmuller W. Peccei D.R and Yanagida T. *Ann. Rev. Nucl. Part. Sci.*, **55**:311, 2005 [hep-ph/0502169].
- [3] Lazarides G. and Shafi Q. *Phys. Lett. B*, **258**:305, 1991.
- [4] Kumekawa K. Moroi T. and Yanagida T. *Prog. Theor. Phys.*, **92**:437, 1994 [hep-ph/9405337].
- [5] Pallis C. and Toumbas N. *J. Cosmol. Astropart. Phys.*, **12**:002, 2011 [arXiv:1108.1771].
- [6] Cervantes-Cota J.L. and Dehnen H. *Nucl. Phys. B*, **442**:391, 1995 [astro-ph/9505069].
- [7] Arai M. Kawai S. and Okada N. *Phys. Rev. D*, **84**:123515, 2011 [arXiv:1107.4767].
- [8] Einhorn B.M. and Jones T.R.D. arXiv:1207.1710.
- [9] Einhorn B.M. and Jones T.R.D. *J. High Energy Phys.*, **03**:026, 2010 [arXiv:0912.2718].
- [10] Lee M.H. *J. Cosmol. Astropart. Phys.*, **08**:003, 2010 [arXiv:1005.2735].
- [11] Ferrara S. Kallosh R. Linde D.A. Marrani A. and Proeyen Van A. *Phys. Rev. D*, **83**:025008, 2011 [arXiv:1008.2942].
- [12] Kallosh R. and Linde D.A. *J. Cosmol. Astropart. Phys.*, **11**:011, 2010 [arXiv:1008.3375].
- [13] Antoniadis I. and Leontaris K.G. *Phys. Lett. B*, **216**:333, 1989.
- [14] Shiu G. and Tye H.-H. S. *Phys. Rev. D*, **58**:106007, 1998.
- [15] Coleman R.S. and Weinberg J.E. *Phys. Rev. D*, **7**:1888, 1973.
- [16] Komatsu E. *et al.* [WMAP Collaboration] *Astrophys. J. Suppl.*, **192**:18, 2011 [arXiv:1001.4538].
- [17] Khlopov Yu. M. and Linde D.A. *Phys. Lett. B*, **138**:265, 1984.
- [18] Bolz M. Brandenburg A. and Buchmüller W. *Nucl. Phys. B*, **606**:518, 2001 [hep-ph/0012052].
- [19] Kawasaki M. Kohri K. and Moroi T. *Phys. Lett. B*, **625**:7, 2005 [astro-ph/0402490].
- [20] Yanagida T. *Proceedings of the Workshop on the Unified Theory and the Baryon Number in the Universe* (O. Sawada and A. Sugamoto, eds.), Tsukuba, Japan, page 95, 1979.
- [21] Gell-Mann M. Ramond P. and Slansky R. *Supergravity* (P. van Nieuwenhuizen *et al.* eds.), North Holland, Amsterdam, page 315, 1979.
- [22] Glashow L.S. *Proceedings of the 1979 Cargese Summer Institute on Quarks and Leptons* (M. Levy *et al.* eds.), page 687, 1980.
- [23] Tortola M. Valle F.W.J. and Vanegas D., arXiv:1205.4018.
- [24] Fogli L.G. Lisi E. Marrone A. Montanino D. Palazzo A. and Rotunno M.A., arXiv:1205.5254.
- [25] Branco C.G. *et al.* *Nucl. Phys. B*, **640**:202, 2002.
- [26] Akhmedov K.E. Frigerio M. and Smirnov Y.A. *J. High Energy Phys.*, **09**:021, 2003 [hep-ph/0305322].

- [27] Šenočuz V.N. *Phys. Rev. D* , **76**:013005, 2007 [arXiv:0704.3048].
- [28] Pallis C. and Shafi Q. *Phys. Rev. D* , in press, 2012 [arXiv:1204.0252].
- [29] Antusch S. Kersten J. Lindner M. and Ratz M. *Nucl. Phys. B* , **674**:401, 2003 [hep-ph/0305273].
- [30] Jeannerot R. Khalil S. Lazarides G. and Shafi Q. *J. High Energy Phys.*, **10**:012, 2000 [hep-ph/0002151].
- [31] King F.S. and Oliveira M. *Phys. Rev. D* , **63**:015010, 2001 [hep-ph/0008183].
- [32] Gogoladze I. Khalid R. Raza S. and Shafi Q. *J. High Energy Phys.*, **12**:055, 2010 [arXiv:1008.2765].
- [33] King F.S. and Oliveira M. *Phys. Rev. D* , **63**:095004, 2001 [hep-ph/0009287].
- [34] Gómez E.M. Lazarides G. and Pallis C. *Nucl. Phys. B* , **638**:165, 2002 [hep-ph/0203131].
- [35] Lazarides G. and Shafi Q. *Phys. Rev. D* , **58**:071702, 1998 [hep-ph/9803397].
- [36] Dimopoulos K. *et al.* *J. High Energy Phys.*, **05**:057, 2003 [hep-ph/0303154].
- [37] Pallis C. and Toumbas N. *J. Cosmol. Astropart. Phys.*, **02**:019, 2011 [arXiv:1101.0325].
- [38] Lyth H.D. and Riotto A. *Phys. Rept.*, **314**:1, 1999 [hep-ph/9807278].
- [39] Lazarides G. *J. Phys. Conf. Ser.*, **53**:528, 2006 [hep-ph/0607032].
- [40] Kofman L. Linde A.D. and Starobinsky A.D. *Phys. Rev. Lett.*, **73**:3195, 1994 [hep-th/9405187].
- [41] Garcia-Bellido J. Figueroa G.D. and Rubio J. *Phys. Rev. D* , **79**:063531, 2009 [arXiv:0812.4624].
- [42] Felder N. Kofman L. and Linde A.D. *Phys. Rev. D* , **59**:123523, 1999 [hep-ph/9812289].
- [43] Endo M. Kawasaki M. Takahashi F. and Yanagida T.T. *Phys. Lett. B* , **642**:518, 2006 [hep-ph/0607170].
- [44] Pallis C. *Nucl. Phys. B* , **751**:129, 2006 [hep-ph/0510234].
- [45] Fukugita M. and Yanagida T. *Phys. Rev. D* , **42**:1285, 1990.
- [46] Ibáñez E.L. and Quevedo F. *Phys. Lett. B* , **283**:261, 1992.
- [47] Baer H. Kraml S. Lessa A. and Sekmen S. *J. Cosmol. Astropart. Phys.*, **04**:039, 2011 [arXiv:1012.3769].
- [48] Kawasaki M. Nakayama K. and Senami M. *J. Cosmol. Astropart. Phys.*, **03**:009, 2008 [arXiv:0711.3083].
- [49] Covi L. Roulet E. and Vissani F. *Phys. Lett. B* , **384**:169, 1996 [hep-ph/9605319].
- [50] Kopp J. *Int. J. Mod. Phys. C* , **19**:523, 2008 [physics/0610206].
- [51] Pallis C. *Phys. Lett. B* , **692**:287, 2010 [arXiv:1002.4765].
- [52] Burgess P.C. Lee M.H. and Trott M. *J. High Energy Phys.*, **09**:103, 2009 [arXiv:0902.4465].
- [53] Barbon F.L.J. and Espinosa R.J. *Phys. Rev. D* , **79**:081302, 2009 [arXiv:0903.0355].
- [54] Bezrukov F. *et al.* *J. High Energy Phys.*, **016**:01, 2011 [arXiv:1008.5157].
- [55] Antusch S. and Spinrath M. *Phys. Rev. D* , **78**:075020, 2008 [arXiv:0804.0717].
- [56] Karagiannakis N. Lazarides G. and Pallis C. *Phys. Lett. B* , **638**:165, 2011 [arXiv:1107.0667].
- [57] Klapdor-Kleingrothaus V. H. *et al.* *Eur. Phys. J. A* , **12**:147, 2001.
- [58] Osipowicz A. *et al.* [KATRIN Collaboration], hep-ex/0109033.